Supporting Information

Stepwise synthesis and catalysis in C-S cross-coupling of pyridine-functionalized N-heterocyclic carbene nickel (II) complexes by mechanochemistry

Xiaoxiao Cui, Xiujia Hao, Fang Guo*
College of Chemistry, Liaoning University, Shenyang 110036, China.
Email: fguo@lnu.edu.cn

Table of contents

Figure S1. Selected bond lengths (Å) and angles (º) for complexes 1-3

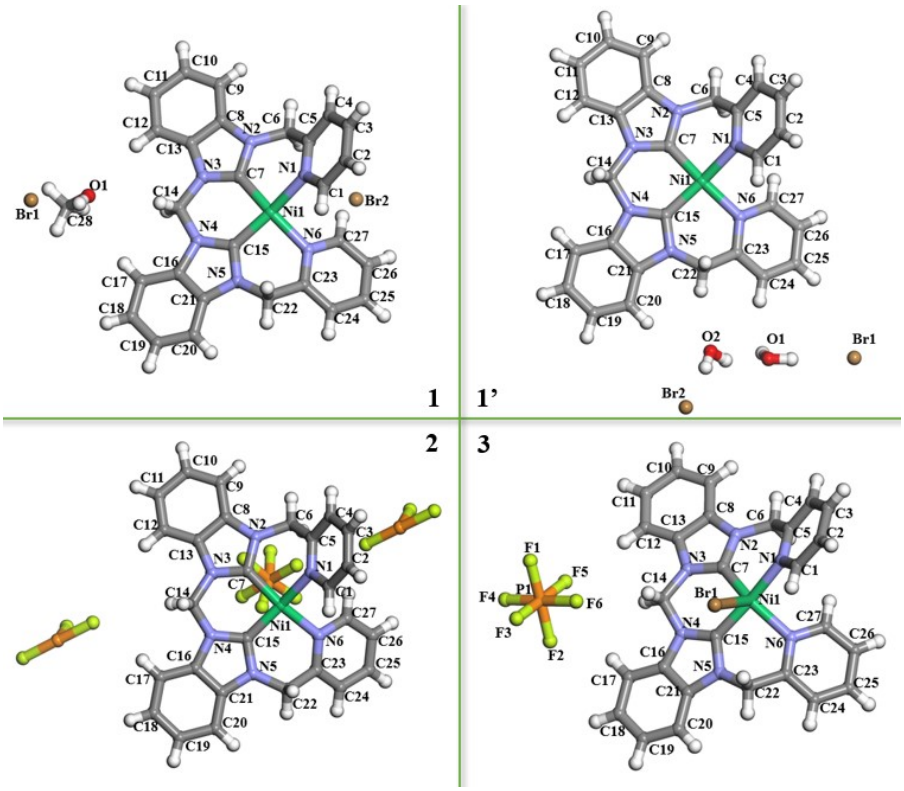

	Bond distances (Å)		Bond angle (°)	
1	N1-Ni1	1.970(3)	∠N1-Ni1-C7	92.22(16)
	C7-Ni1	1.851(4)	∠C7-Ni1-C15	88.97(18)
	C15-Ni1	1.851(4)	∠C15-Ni1-N6	92.36(16)
	N6-Ni1	1.952(3)	∠N6-Ni1-N1	92.34(14)
1'	N1-Ni1	1.959(5)	∠N1-Ni1-C7	91.10(2)
	C7-Ni1	1.860(6)	∠C7-Ni1-C15	88.80(3)
	C15-Ni1	1.865(6)	∠C15-Ni1-N6	93.40(2)
	N6-Ni1	1.962(5)	∠N6-Ni1-N1	92.30(2)
2	N1-Ni1	1.929(5)	∠N1-Ni1-C7	90.20(2)
	C7-Ni1	1.842(6)	∠C7-Ni1-C15	89.30(3)
	C15-Ni1	1.852(6)	∠C15-Ni1-N6	93.90(2)
	N6-Ni1	1.938(5)	∠N6-Ni1-N1	93.80(2)
3	N1-Ni1	1.959(3)	∠N1-Ni1-C7	91.41(12)
	C7-Ni1	1.850(3)	∠C7-Ni1-C15	88.35(13)
	C15-Ni1	1.859(3)	∠C15-Ni1-N6	92.32(12)
	N6-Ni1	2.018(3)	∠N6-Ni1-N1	91.61(12)
	Br-Ni1	2.8536(6)		

Figure S2. Hydrogen bonding data of complex 1

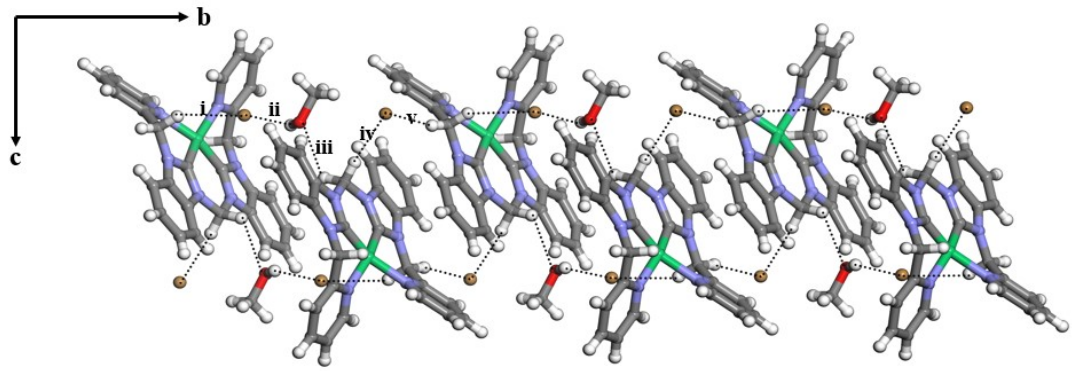

D-H···A	D-H (Å)	H···A (Å)	D···A (Å)	D-H···A (°)	Symmetry Code
C22-H22B····Br1(i)	0.970	2.737	3.512	137.33	-x+1, -y+1, -z+1
O1-H1A···Br1(ii)	0.820	2.534	3.274	150.70	x, y, z
C14-H14A···O1(iii)	0.970	2.683	3.365	127.80	x, y, z
C14-H14B···Br2(iv)	0.970	2.830	3.770	163.39	-x+2, -y, -z+1
C22-H22A···Br2(v)	0.970	2.682	3.633	166.75	-x+1, -y+1, -z+1

Figure S3. Hydrogen bonding data of complex 1'

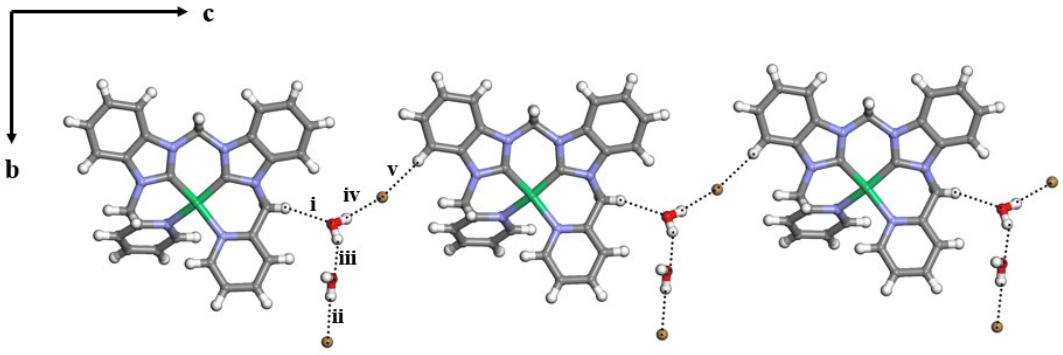

D-H···A	D-H (Å)	H···A (Å)	D···A (Å)	D-H···A (°)	Symmetry Code
C22-H22B····O2(i)	0.895	2.455	3.321	163.27	x, y, z
O1-H1B···Br1(ii)	0.850	2.479	3.310	166.02	x, y, z
O2-H2B···O1(iii)	0.850	2.007	2.801	154.98	-x+1, -y+1, -z+1

O2-H2A···Br2(iv)	0.849	2.472	3.315	172.01	x, y, z
C9-H9···Br2(v)	0.930	2.931	3.747	147.17	x-1, y, z-1

Figure S4. Hydrogen bonding data of complex 2

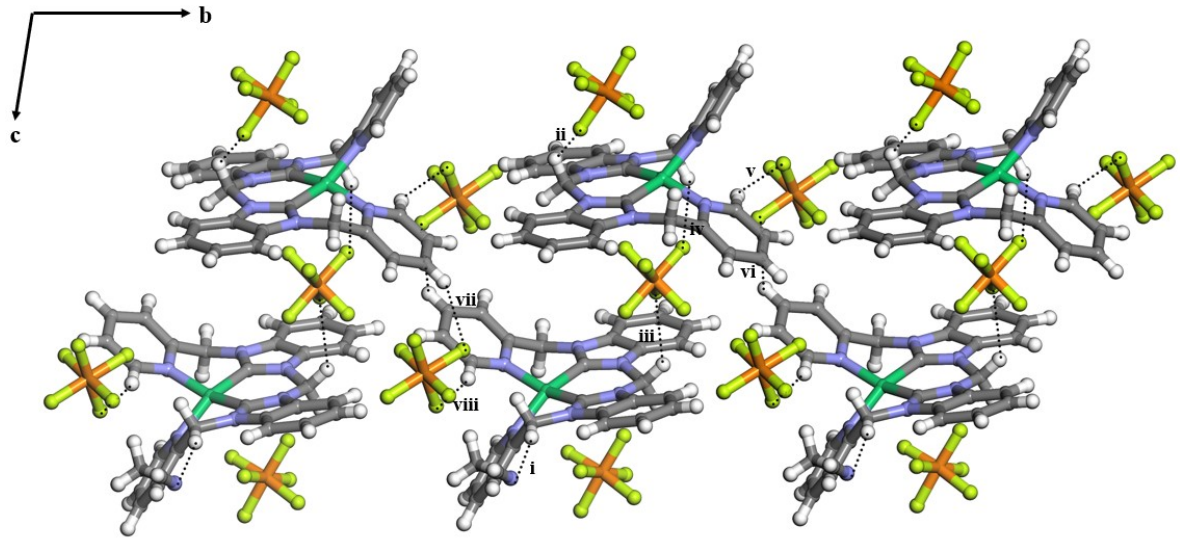

D-H···A	D-H (Å)	H···A (Å)	D···A (Å)	D-H···A (°)	Symmetry Code
C3-H33B···N13(i)	1.090	2.462	3.288	131.61	x, y, z
C14-H14A···F1(ii)	0.970	2.526	3.161	123.03	-x+1, y, -z+1
C41-H41B···F9(iii)	0.971	2.580	3.263	127.47	x, y, z
C6-H6B···F8(iv)	0.970	2.459	3.305	145.59	x, y, z
C27-H27···F20(v)	0.930	2.504	3.303	144.19	-x+1, y, -z+2
C52-H52···F21(vi)	0.930	2.512	3.279	139.95	x, y, z
C25-H25···F22(vii)	0.930	2.530	3.369	150.27	x, y, z
C54-H54···F23(viii)	0.929	2.394	3.268	156.58	-x+3/2, y-1/2, -z+2

Figure S5. Hydrogen bonding data of complex 3

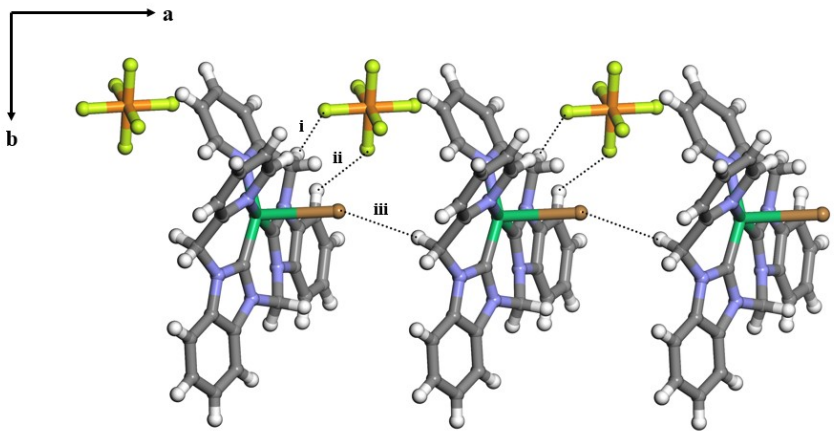

D-H···A	D-H (Å)	H···A (Å)	D···A (Å)	D-H···A (°)	Symmetry Code
C22-H22A···F3(i)	0.970	2.474	3.402	160.18	-x+2, -y+1, -z+1
C20-H20···F4(ii)（ii）	0.930	2.455	3.199	137.04	-x+2, -y+1, -z+1
C6-H6B···Br1(iii)	0.970	2.950	3.820	149.84	x-1, y, z

Figure S6. The overlapping of complex 1, 2 and 3

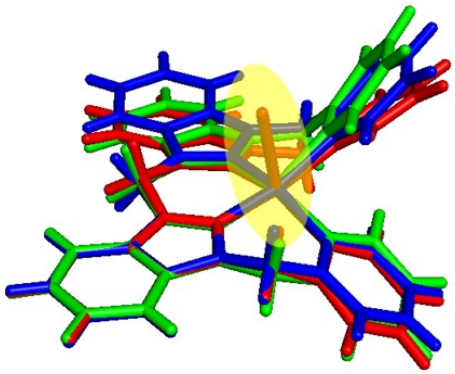

complex **1**, blue; complex **2**, green; complex **3**, red.

Figure S7. PXRD data of complex 1

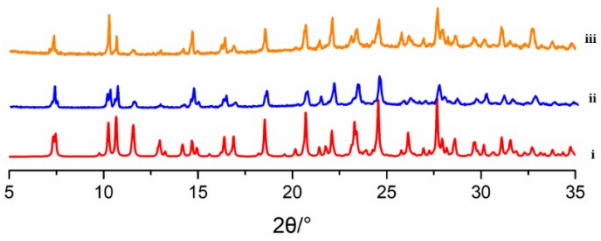

Simulated PXRD pattern from single crystal **1** (**i**), recrystallization of the grinding product (**ii**), and grinding product of **$[H_2L]Br_2$** with equal moles of $Ni(OAc)_2$ (**iii**).

Figure S8. PXRD data of complex 1'

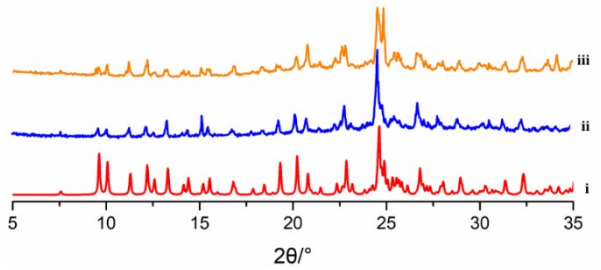

Simulated PXRD pattern from single crystal **1'** (**i**), recrystallization of the grinding product (**ii**), and grinding product of **$[H_2L]Br_2$** with equal moles of $Ni(OAc)_2$ (**iii**).

Figure S9. PXRD data of complex 2

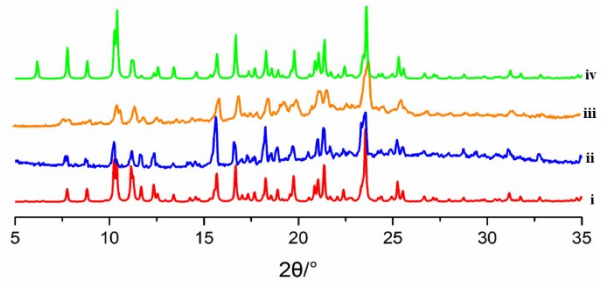

Simulated PXRD pattern of single crystal **2** (**i**), recrystallization of the grinding product (**ii**), grinding product of **$[H_2L](PF_6)_2$** with equal moles of $Ni(OAc)_2$ (**iii**), and Crystals reported in the Organometallics 2007, 26, 6636–6642, CSDcode:XIVSEB (**iv**) (Note: the characteristic peak at 2θ=6° is the main difference between complex 2 and reported structure, which reduced the sapce group from the C2/c to C2 due to the involvent of solvent.)

Figure S10. PXRD data of complex 3

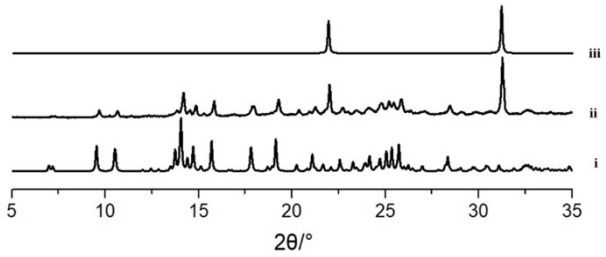

Simulated PXRD pattern from single crystal **3** (**i**), grinding product of **2** and KBr (**ii**), simulated PXRD of KPF_6, ICSD 25576 (**iii**)

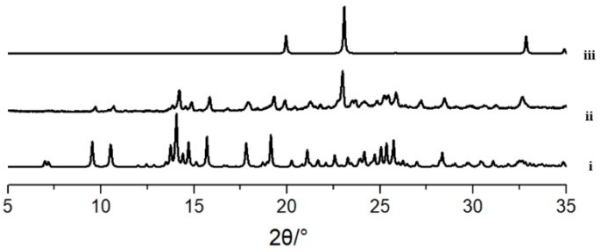

Simulated PXRD pattern from single crystal **3** (**i**), grinding product of **1/1'** and NH_4PF_6 (**ii**), simulated PXRD of NH_4Br, ICSD 53838 (**iii**)

Figure S11. ^{1}H NMR data of 2-(benzo[d]thiazol-2-ylthio)-1-phenylethanone recrystallized from ethanol

Synthetic method: A mixture of 2-bromoacetophenone (1 mmol, 0.199 g), 2-mercaptobenzothiazole (1 mmol, 0.167 g), $[NiLBr]PF_6$ (**3**) (0.018 mmol, 0.0123 mg), and methanol (30 μL) was ground together with a pestle in an agate mortar at room temperature for 30 min. The grinding powder was completely dissolved in an ethanol solution (6 ml), and left for 1-2 days, giving rise to colorless needle crystal, Yield: 92%.

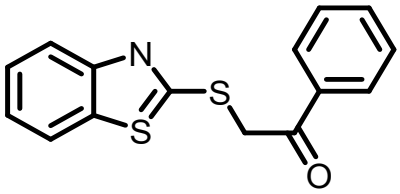

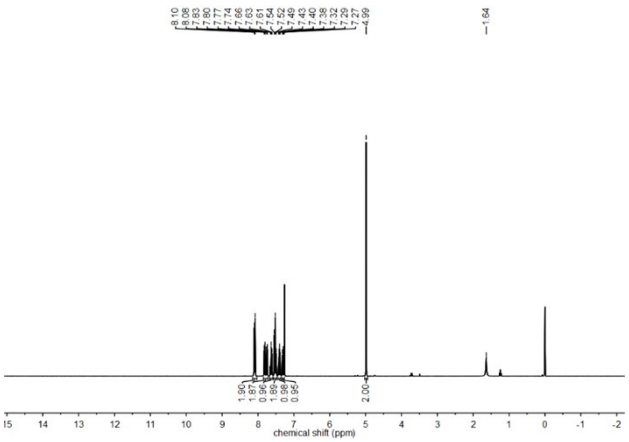

Recrystallized product from ethanol：**^{1}H NMR** (300 MHz, $CDCl_3$) δ = 8.09 (d, *J* = 7.1 Hz, 2H), 7.78 (dd, *J* = 19.4, 8.0 Hz, 2H), 7.63 (t, *J* = 6.8 Hz, 1H), 7.52 (t, *J* = 7.5 Hz, 2H), 7.40 (t, *J* = 7.1 Hz, 1H), 7.33 – 7.27 (m, 1H), 4.99 (s, 2H).

Figure S12. PXRD data of 2-(benzo[d]thiazol-2-ylthio)-1-phenylethanone recrystallized from ethanol

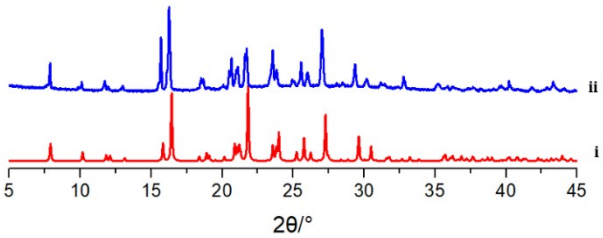

Simulated PXRD pattern from 2-(benzo[d]thiazol-2-ylthio)-1-phenylethanone (CSD code: PUFGED and PUFGED01) (**i**); Crystals recrystallized from ethanol (**ii**)

Table S1. Crystal data and structural refinement parameters for complexes 1-3

Crystal	**1**	**1'**	**2**	**3**
Empirical formula	$C_{28}H_{26}Br_2N_6NiO$	$C_{27}H_{26}Br_2N_6NiO_2$	$C_{56}H_{47}F_{24}N_{13}Ni_2P_4$	$C_{27}H_{22}BrF_6N_6NiP$
Formula weight	681.08	685.07	1599.36	714.09
Crystal system	triclinic	triclinic	Monoclinic	triclinic
Space group	*P-1*	*P-1*	*C2*	*P-1*
Z	2	2	4	2
a (Å)	9.1629(7)	8.0554(8)	31.2054(15)	8.4515(4)
b (Å)	11.9336(10)	11.9275(12)	12.4113(6)	12.4422(6)
c (Å)	12.1402(9)	14.1463(13)	17.2760(9)	12.7049(7)

α (deg)	91.507(4)	91.319(4)	90	95.299(2)
β (deg)	96.448(4)	95.998(4)	113.261(2)	91.357(2)
γ (deg)	96.523(4)	102.033(4)	90	96.987(2)
V (Å3)	1309.52(18)	1320.6(2)	6147.1(5)	1319.57(12)
Dx ($Mg.cm^{-3}$)	1.727	1.723	1.728	1.797
μ (mm^{-1})	3.827	3.798	0.842	2.384
F (000)	684.0	688.0	3224.0	716
R_{int}	0.0627	0.0401	0.0296	0.0464
No.of collected data(unique)	21435	21263	49237	22874
No.of data with I>2σ (I)	3965	4881	12360	4878
No.of parameter	345	358	895	379
S	1.109	1.192	1.053	1.049
R1	0.0685	0.0653	0.0511	0.0474
wR2	0.0974	0.1692	0.1325	0.1113

Table S2. Parallel experiment of catalyst screening

Cat.	First yield (%)	Second yield (%)	Third yield (%)	Average yield (%)
1	36	38	36	37
1'	32	33	30	32
2	42	40	39	41
3	47	45	46	46

Reaction conditions: 2-bromoacetophenone (1 mmol), 2-mercaptobenzothiazole (1 mmol) and 0.6 mol% of Ni-NHC, grinding. Isolated yields after silica gel column chromatography.

Table S3. Solution-based C-S cross-coupling reaction using complex 3 as catalyst

Entry	Time(min)	Solution	Yield (%)
1	20	CH_3OH	18
2	30	CH_3OH	25
3	40	CH_3OH	7

Reaction conditions: 2-bromoacetophenone (1 mmol), 2-mercaptobenzothiazole (1 mmol) and 1.8 mol% of complex **3**, CH_3OH (8 mL), stirring. Isolated yields after silica gel column chromatography.

Table S4 Substrate scope for the catalyst complex 3

product	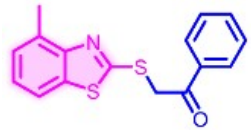	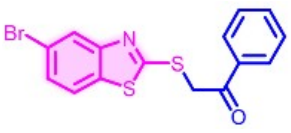	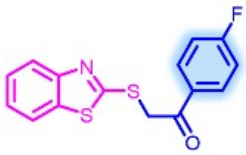	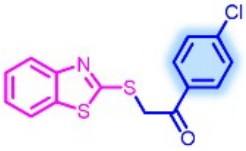
yield	**73%**	**43%**	**83%**	**25%**
product	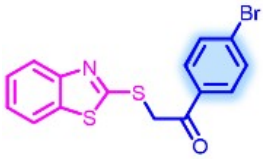	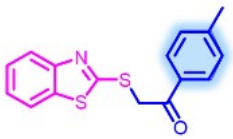	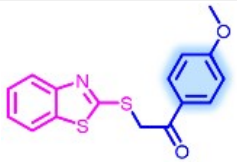	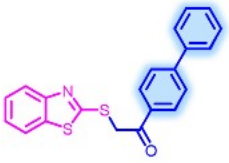
yield	**21%**	**88%**	**37%**	**16%**

Reaction conditions: phenacyl bromides (1 mmol), 2-mercaptobenzothiazoles (1 mmol), 1.8 mol% of complex **3**, grinding aid CH_3OH (30 μL). Isolated yields after silica gel column chromatography

Table S5. E-factor for the C-S cross-coupling catalyst system

Entry	Input Amount	Out Amount
1	2-bromoacetophenone 0.199 g	2-(benzo[d]thiazol-2-ylthio)-1-phenylethanone 0.265 g,
2	2-mercaptobenzothiazole 0.167 g	-
3	$[NiLBr]PF_6$ (**3**) 0.013 g	-
4	Methanol 0.024 g	-
	Total 0.403 g	Total 0.265 g

$$E\text{—}Factor = \frac{\text{Amount of waste}}{\text{Amount of product}} = \frac{0.403 - 0.265}{0.265} = 0.520 \quad (1.1)$$

Table S6. EcoScale penalty points for the C-S cross-coupling catalyst system

EcoScale penalty points	Factor	Penalty
1. Yield	93%	3.5
2. Price	2-bromoacetophenone	0
	2-mercaptobenzothiazole	0
	$MgSO_4$	0
3. Safety	2-mercaptobenzothiazole (N)	5
	petroleum ether (F)	5
4. Technical setup	agate mortar	0

5. Temperature /time	room temperature, 30 min	0
6. Workup and purification	classic chromatography	10
Penalty points total		**23.5**

EcoScale = 100 - sum of individual penalties = 100 – 23.5 = 76.5

Table S7. Elemental analysis of complexes 1-3

Entry	Anal. calcd			Found		
	C	H	N	C	H	N
1	49.33	3.82	12.33	49.29	3.80	12.26
1'	47.29	3.80	12.26	47.31	3.82	12.23
2	42.02	2.94	11.38	42.06	2.91	11.41
3	45.37	3.08	11.76	45.38	3.11	11.71

Figure S13. Elemental analysis chromatograms of complexes 1-3

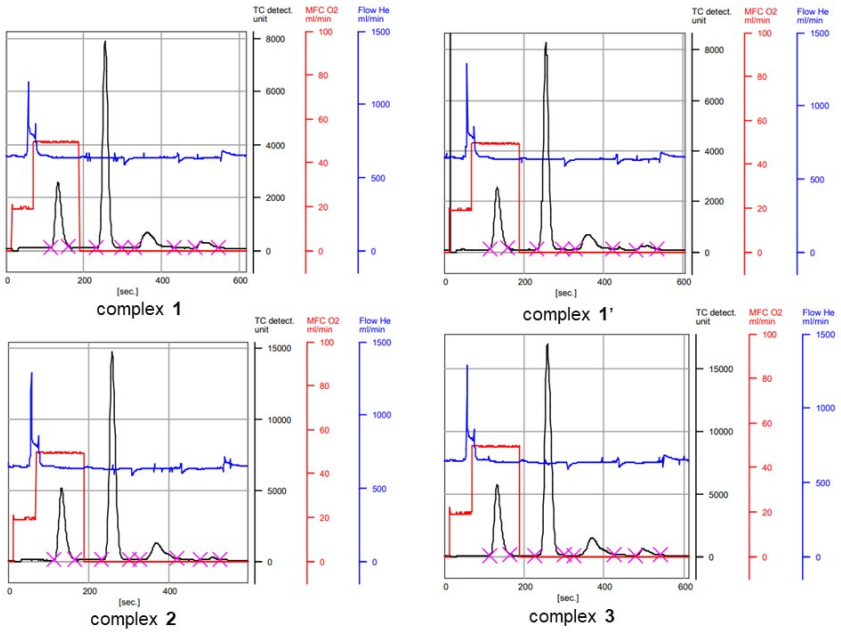

Analytical Data of Products

$[H_2L]Br_2$

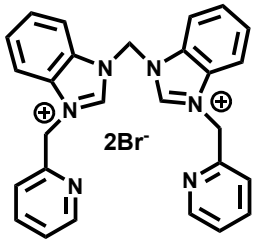

^{1}H NMR (300 MHz, DMSO) δ = 10.65 (s, 2H), 8.46 (d, *J* = 4.5 Hz, 2H), 8.40 (d, *J* = 8.3 Hz, 2H), 8.04 (d, *J* = 8.2 Hz, 2H), 7.92 (t, *J* = 7.7 Hz, 2H), 7.74 (dq, *J* = 14.8, 7.5 Hz, 6H), 7.60 (s, 2H), 7.44 – 7.35 (m, 2H), 6.05 (s, 4H).

$[H_2L](PF_6)_2$

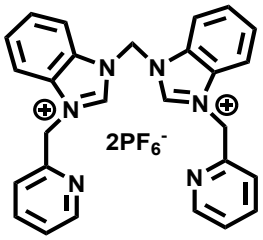

^{1}H NMR (300 MHz, DMSO) δ = 10.51 (s, 2H), 8.47 (d, J = 4.5 Hz, 2H), 8.36 (d, J = 8.3 Hz, 2H), 8.05 (d, J = 8.2 Hz, 2H), 7.93 (t, J = 7.7 Hz, 2H), 7.80 (t, J = 7.7 Hz, 2H), 7.72 (dt, J = 7.4, 3.6 Hz, 4H), 7.53 (s, 2H), 7.44 – 7.36 (m, 2H), 6.02 (s, 4H))

$[NiL]Br_2 \cdot CH_3OH$ (1)

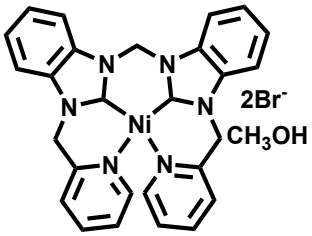

^{1}H NMR (400 MHz, DMSO) δ = 8.79 (d, *J* = 5.9 Hz, 2H), 8.27 (t, *J* = 7.0 Hz, 2H), 8.20 – 8.10 (m, 4H), 8.02 (d, *J* = 7.8 Hz, 2H), 7.71 – 7.63 (m, 4H), 7.60 (t, *J* = 6.5 Hz, 2H), 6.95 (s, 2H), 6.18 (s, 4H).

$[NiL]Br_2 \cdot 2H_2O$ (1')

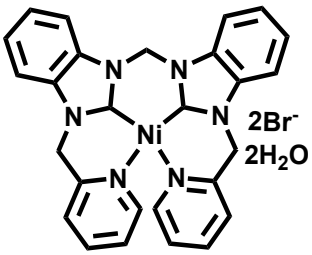

^{1}H NMR (400 MHz, DMSO) δ = 8.78 (d, *J* = 5.2 Hz, 2H), 8.25 (td, *J* = 7.7, 1.4 Hz, 2H), 8.20 – 8.08 (m, 4H), 8.01 (d, *J* = 7.5 Hz, 2H), 7.70 – 7.62 (m, 4H), 7.61 – 7.54 (m, 2H), 6.94 (s, 2H), 6.17 (s, 4H).

[NiL](PF$_6$)$_2$·0.5CH$_3$CN (2)

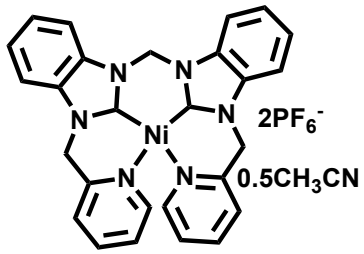

^{1}H NMR (400 MHz, DMSO) δ = 8.74 (d, *J* = 5.8 Hz, 2H), 8.35 (td, *J* = 7.7, 1.5 Hz, 2H), 8.22 (dd, *J* = 6.1, 3.0 Hz, 2H), 8.17 (d, *J* = 2.1 Hz, 2H), 8.07 (d, *J* = 7.5 Hz, 2H), 7.79 – 7.72 (m, 4H), 7.68 (t, *J* = 6.7 Hz, 2H), 7.08 (s, 2H), 6.23 (s, 4H).

[NiLBr]PF$_6$ (3).

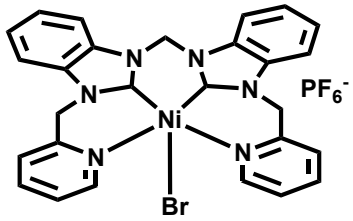

^{1}H NMR (400 MHz, DMSO) δ = 8.78 (d, *J* = 5.6 Hz, 2H), 8.26 (t, *J* = 7.7 Hz, 2H), 8.21 – 8.07 (m, 4H), 8.02 (d, *J* = 7.6 Hz, 2H), 7.74 – 7.62 (m, 4H), 7.60 (t, *J* = 6.5 Hz, 2H), 6.95 (s, 2H), 6.17 (s, 4H).

2-(benzo[d]thiazol-2-ylthio)-1-phenylethanone: White solid; yield: 93%.

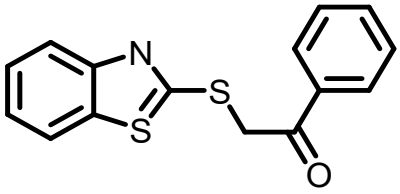

^{1}H NMR (300 MHz, $CDCl_3$) δ = 8.09 (d, *J* = 7.5 Hz, 2H), 7.78 (d, *J* = 19.7, 7.8 Hz, 2H), 7.63 (t, *J* = 7.4 Hz, 1H), 7.52 (t, *J* = 7.7 Hz, 2H), 7.40 (t, *J* = 7.4 Hz, 1H), 7.33 – 7.24 (m, 1H), 4.98 (s, 2H). **^{13}C NMR** (75 MHz, $CDCl_3$) δ = 192.75 (s), 165.10 (s), 152.69 (s), 135.31 (d, *J* = 4.6 Hz), 133.69 (s), 129.06 (s), 128.53 (d, *J* = 18.2 Hz), 125.89 (s), 124.25 (s), 121.33 (s), 120.94 (s), 40.92 (s). **IR** (KBr): ν = 1597.43 cm^{-1} (C=O).

2-(benzo[d]thiazol-2-ylthio)-1-(4-fluorophenyl)ethenone : White solid; yield: 83%.

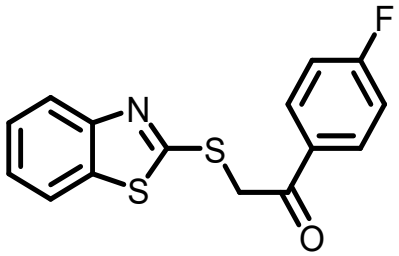

^{1}H NMR (300 MHz, $CDCl_3$) δ = 8.12 (dd, *J* = 8.8, 5.4 Hz, 2H), 7.78 (dd, *J* = 17.0, 8.0 Hz, 2H), 7.40 (t, *J* = 7.2 Hz, 1H), 7.34 – 7.24 (m, 1H), 7.18 (t, *J* = 8.6 Hz, 2H), 4.93 (s, 2H). **^{13}C NMR** (100 MHz, $CDCl_3$) δ = 190.48 (s), 165.24 (d, *J* = 235 Hz), 164.07 (s), 151.73 (s), 134.49 (s),

130.94 (d, *J* = 3.1 Hz), 130.32 (d, *J* = 9.5 Hz), 125.06 (s), 123.46 (s), 120.45 (s), 120.09 (s), 114.96 (d, *J* = 22.2 Hz), 39.61 (s). **IR** (KBr): ν = 1597.33 cm^{-1} (C=O).

2-(benzo[d]thiazol-2-ylthio)-1-(4-chlorophenyl)ethenone : White solid; yield: 25%.

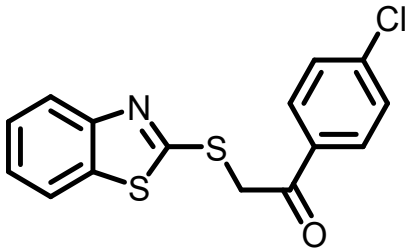

^{1}H NMR (300 MHz, DMSO) δ = 8.10 (d, *J* = 8.6 Hz, 2H), 8.00 (d, *J* = 7.9 Hz, 1H), 7.74 (d, *J* = 7.9 Hz, 1H), 7.66 (d, *J* = 8.6 Hz, 2H), 7.43 (t, *J* = 7.6 Hz, 1H), 7.39 – 7.30 (m, 1H), 5.14 (s, 2H). **^{13}C NMR** (75 MHz, DMSO) δ = 192.21 (s), 165.79 (s), 152.51 (s), 138.83 (s), 134.86 (s), 134.21 (s), 130.49 (s), 129.09 (s), 126.46 (s), 124.61 (s), 121.95 (s), 121.14 (s), 40.93 (s). **IR** (KBr): ν = 1598.16 cm^{-1} (C=O).

2-(benzo[d]thiazol-2-ylthio)-1-(4-bromophenyl)ethanone : White solid; yield: 21%.

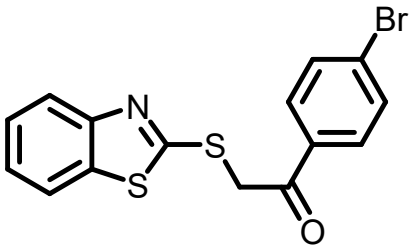

^{1}H NMR (300 MHz, $CDCl_3$) δ = 7.96 (d, *J* = 8.6 Hz, 2H), 7.78 (dd, *J* = 13.4, 8.0 Hz, 2H), 7.66 (d, *J* = 8.6 Hz, 2H), 7.40 (t, *J* = 7.7 Hz, 1H), 7.29 (t, *J* = 12.3 Hz, 2H), 4.91 (s, 2H). **^{13}C NMR** (75 MHz, $CDCl_3$) δ = 192.16 (s), 164.88 (s), 152.69 (s), 135.49 (s), 134.20 (s), 132.11 (s), 130.07 (s), 129.12 (s), 126.06 (s), 124.46 (s), 121.44 (s), 121.10 (s), 40.49 (s). **IR** (KBr): ν = 1598.25 cm^{-1} (C=O).

2-(benzo[d]thiazol-2-ylthio)-1-p-tolylethanone : yellow solid; yield: 88%.

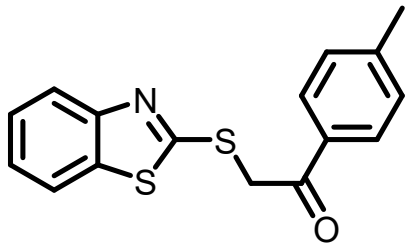

^{1}H NMR (300 MHz, $CDCl_3$) δ = 7.97 (d, *J* = 8.2 Hz, 2H), 7.82 (d, *J* = 8.0 Hz, 1H), 7.74 (d, *J* = 8.0 Hz, 1H), 7.39 (t, *J* = 8.2 Hz, 1H), 7.28 (t, *J* = 8.4 Hz, 3H), 4.95 (s, 2H), 2.43 (s, 3H). **^{13}C NMR** (75 MHz, $CDCl_3$) δ = 192.28 (s), 165.26 (s), 152.72 (s), 144.69 (s), 135.31 (s), 132.73 (s), 129.32 (s), 128.52 (s), 125.86 (s), 124.75 (s), 124.21 (s), 121.30 (s), 120.91 (s), 40.94 (s), 21.62 (s). **IR** (KBr): ν = 1599.15 cm^{-1} (C=O).

2-(benzo[d]thiazol-2-ylthio)-1-(4-methoxyphenyl)ethenone : White solid; yield: 37%.

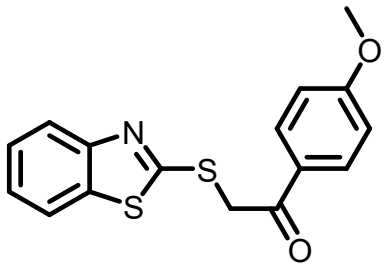

^{1}H NMR (300 MHz, DMSO) δ = 8.04 (d, *J* = 20.8, 8.4 Hz, 3H), 7.78 (d, *J* = 8.0 Hz, 1H), 7.40 (dt, *J* = 15.8, 7.3 Hz, 2H), 7.11 (d, *J* = 8.8 Hz, 2H), 5.12 (s, 2H), 3.88 (s, 3H). **^{13}C NMR** (75 MHz, DMSO) δ = 191.20 (s), 166.12 (s), 163.72 (s), 152.61 (s), 134.83 (s), 131.36 (s), 130.98 (s), 128.27 (s), 126.42 (s), 124.53 (s), 121.88 (s), 121.13 (s), 114.17 (s), 55.73 (s), 40.83 (s). **IR** (KBr): ν = 1595.30 cm^{-1} (C=O).

1-([1,1'-biphenyl]-4-yl)-2-(benzo[d]thiazol-2-ylthio)ethanone: White solid; yield: 16%.

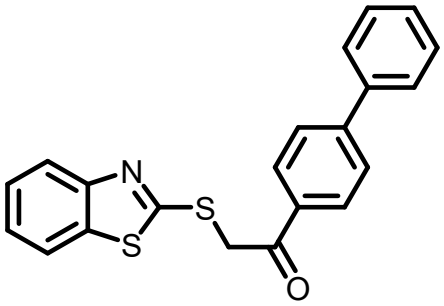

^{1}H NMR (300 MHz, $CDCl_3$) δ = 8.15 (d, *J* = 8.4 Hz, 2H), 7.83 (d, *J* = 7.8 Hz, 1H), 7.74 (t, *J* = 7.6 Hz, 3H), 7.64 (d, *J* = 7.9 Hz, 2H), 7.44 (dt, *J* = 18.7, 7.6 Hz, 4H), 7.28 (dd, *J* = 13.4, 6.3 Hz, 1H), 5.00 (s, 2H). **^{13}C NMR** (75 MHz, $CDCl_3$) δ = 192.50 (s), 165.30 (s), 152.75 (s), 146.50 (s), 139.59 (s), 135.45 (s), 134.08 (s), 129.09 (d, *J* = 16.3 Hz), 128.41 (s), 127.43 (t, *J* = 13.4 Hz), 126.04 (s), 124.29 (d, *J* = 17.5 Hz), 121.45 (s), 121.07 (s), 40.98 (s). **IR** (KBr): ν = 1600.00 cm^{-1} (C=O).

2-(4-methylbenzo[d]thiazol-2-ylthio)-1-phenylethanone: White solid; yield: 73%.

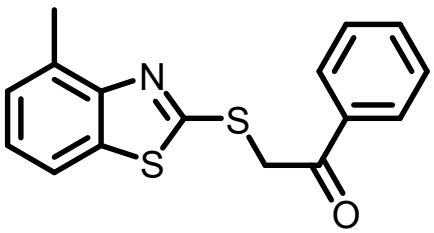

^{1}H NMR (300 MHz, DMSO) δ = 8.10 (d, *J* = 7.2 Hz, 2H), 7.84 – 7.74 (m, 1H), 7.70 (t, *J* = 7.4 Hz, 1H), 7.58 (t, *J* = 7.5 Hz, 2H), 7.20 (d, *J* = 9.4 Hz, 2H), 5.08 (s, 2H), 3.33 (s, 3H). **^{13}C NMR** (75 MHz, DMSO) δ = 193.33 (s), 164.48 (s), 151.65 (s), 135.82 (s), 134.70 (s), 133.78 (s), 130.61 (s), 128.91 (s), 128.49 (s), 126.82 (s), 124.52 (s), 119.24 (s), 17.65 (s). **IR** (KBr): ν = 1595.42 cm^{-1} (C=O).

2-(5-bromobenzo[d]thiazol-2-ylthio)-1-phenylethanone: White solid; yield: 43%.

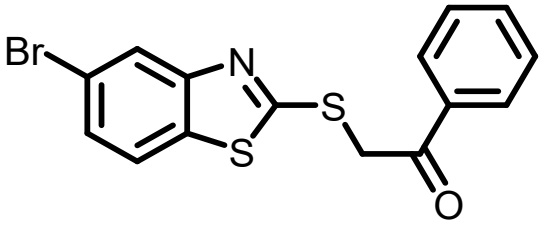

^{1}H NMR (300 MHz, DMSO) δ = 8.30 (d, *J* = 2.0 Hz, 1H), 8.09 (d, *J* = 7.2 Hz, 2H), 7.71 (dd, *J* = 12.7, 7.5 Hz, 2H), 7.60 (t, *J* = 7.6 Hz, 3H), 5.19 (s, 2H). **^{13}C NMR** (75 MHz, DMSO) δ = 192.85 (s), 167.41 (s), 151.64 (s), 136.85 (s), 135.40 (s), 133.95 (s), 129.51 (s), 128.97 (s), 128.55 (s), 124.45 (s), 122.52 (s), 116.99 (s), 41.21 (s). **IR** (KBr): ν = 1598.19 cm^{-1} (C=O).

Spectra of Products

Figure S1. ^{1}**H NMR** spectrum of $[H_2L]Br_2$

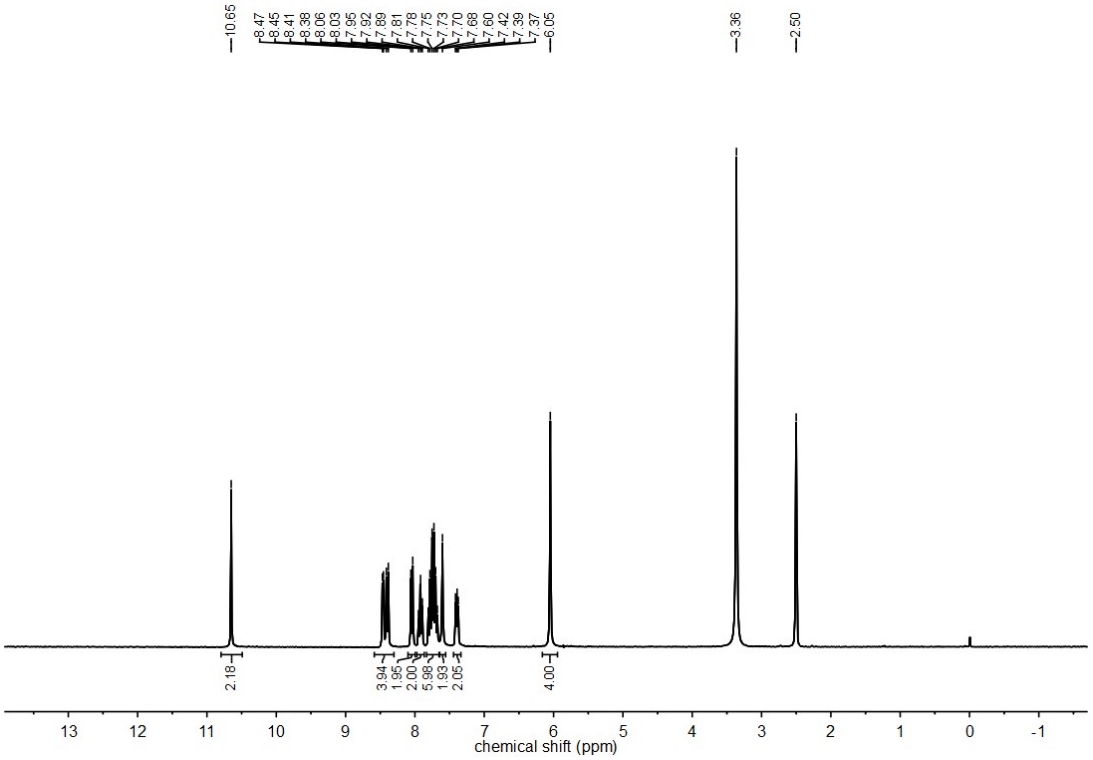

Figure S2. ^{1}**H NMR** spectrum of $[H_2L](PF_6)_2$

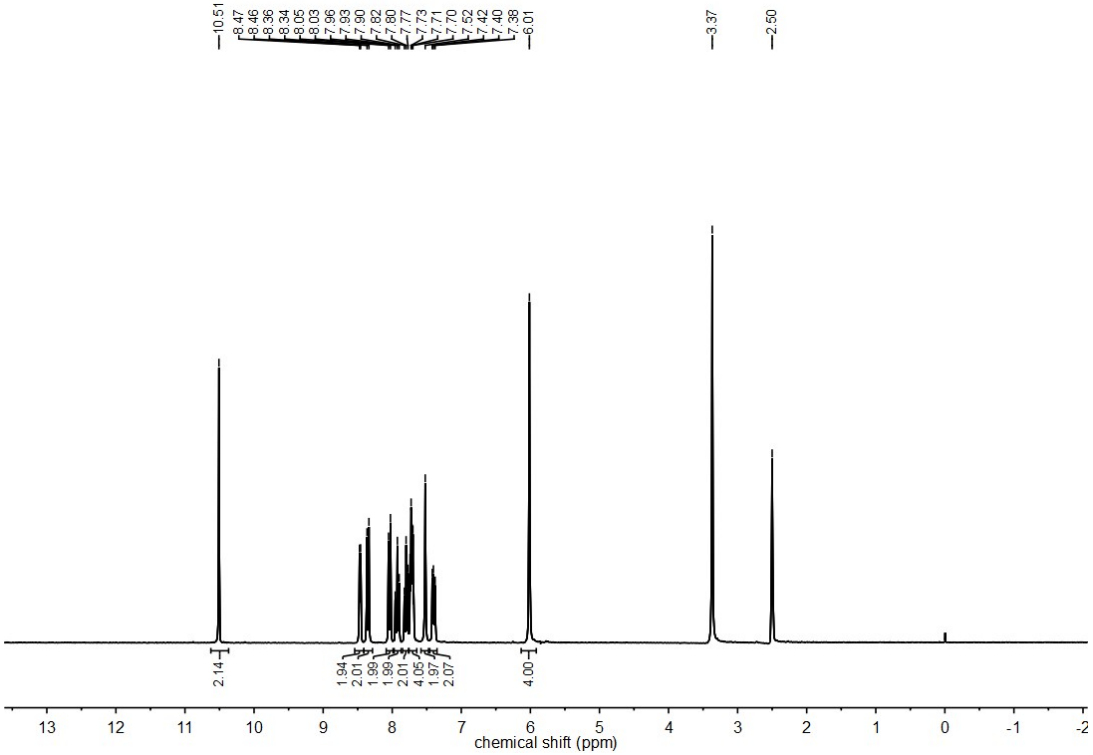

Figure S3. ^{1}**H NMR** spectrum of **[NiL]Br_2·CH_3OH (1)**

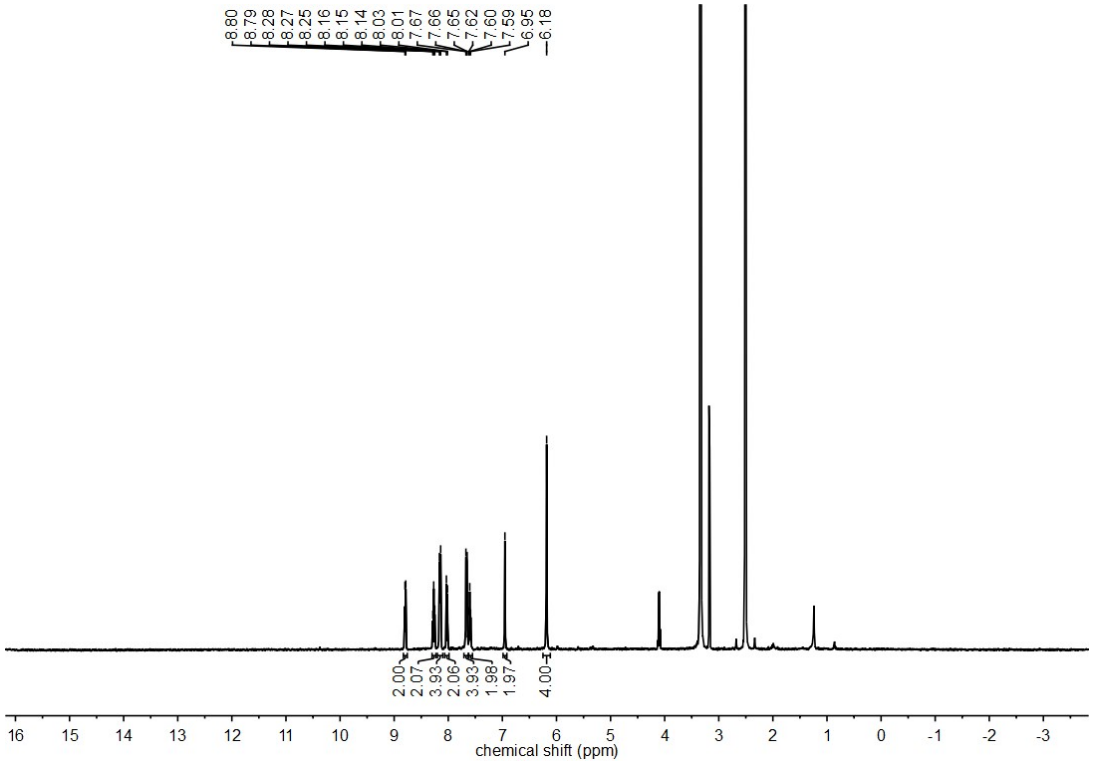

Figure S4. ^{1}**H NMR** spectrum of **[NiL]Br_2·$2H_2O$ (1')**

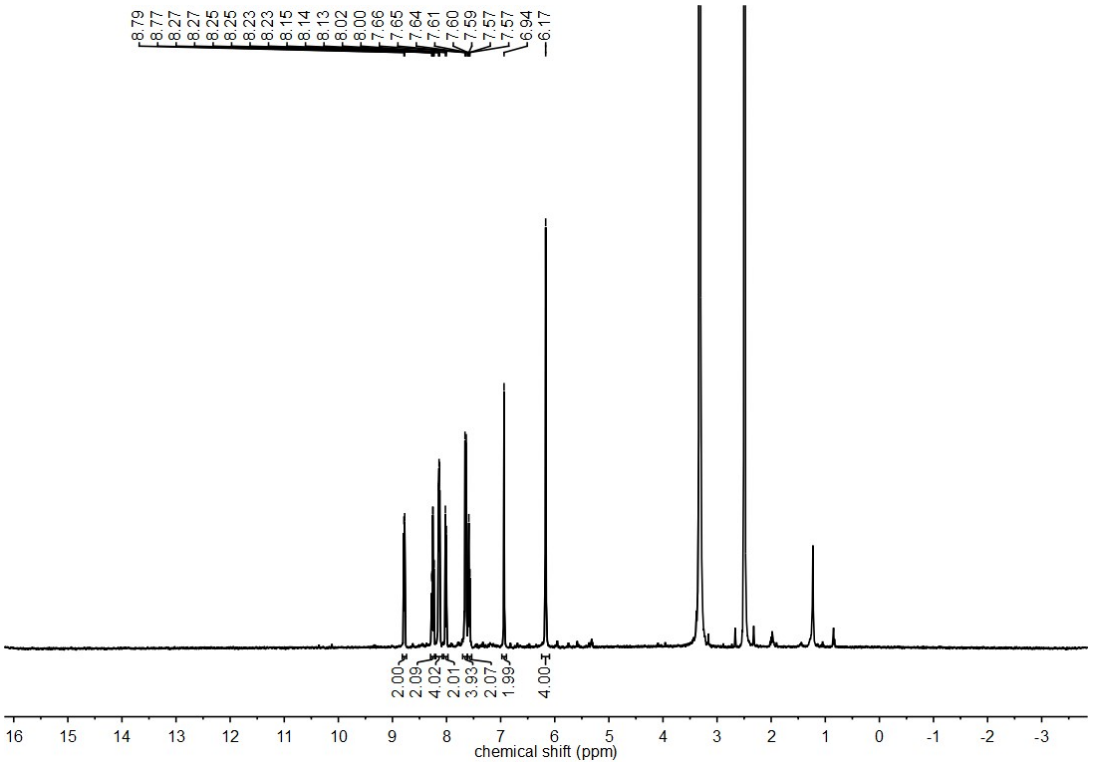

Figure S5. ^{1}**H NMR** spectrum of **[NiL](PF$_6$)$_2$·0.5CH$_3$CN (2)**

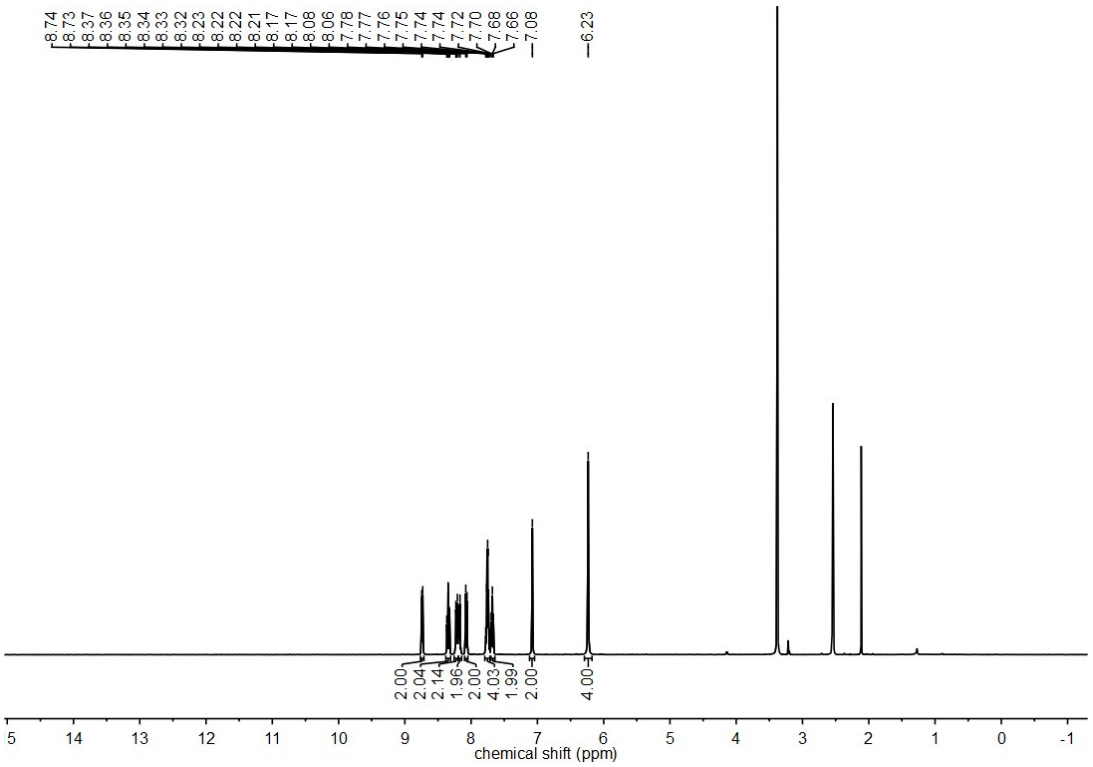

Figure S6. ^{1}**H NMR** spectrum of **[NiLBr]PF$_6$ (3)**

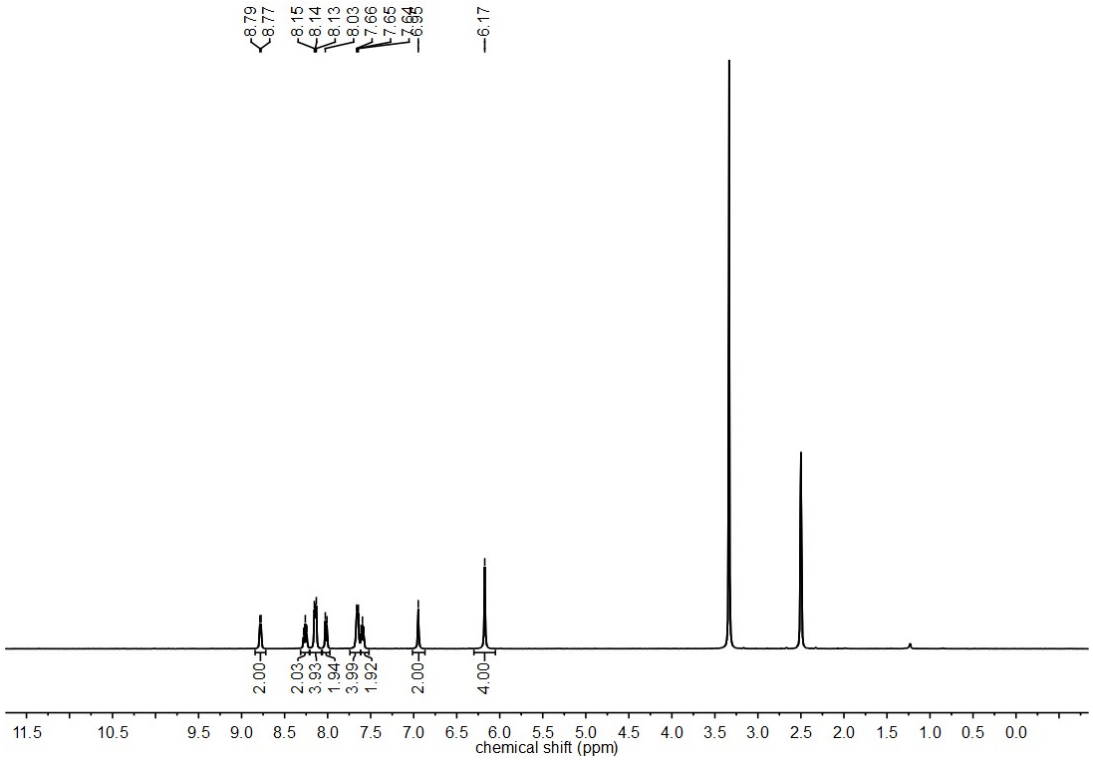

Figure S7. ^{1}H NMR and **^{13}C NM**R spectrum of 2-(benzo[d]thiazol-2-ylthio)-1-phenylethanone

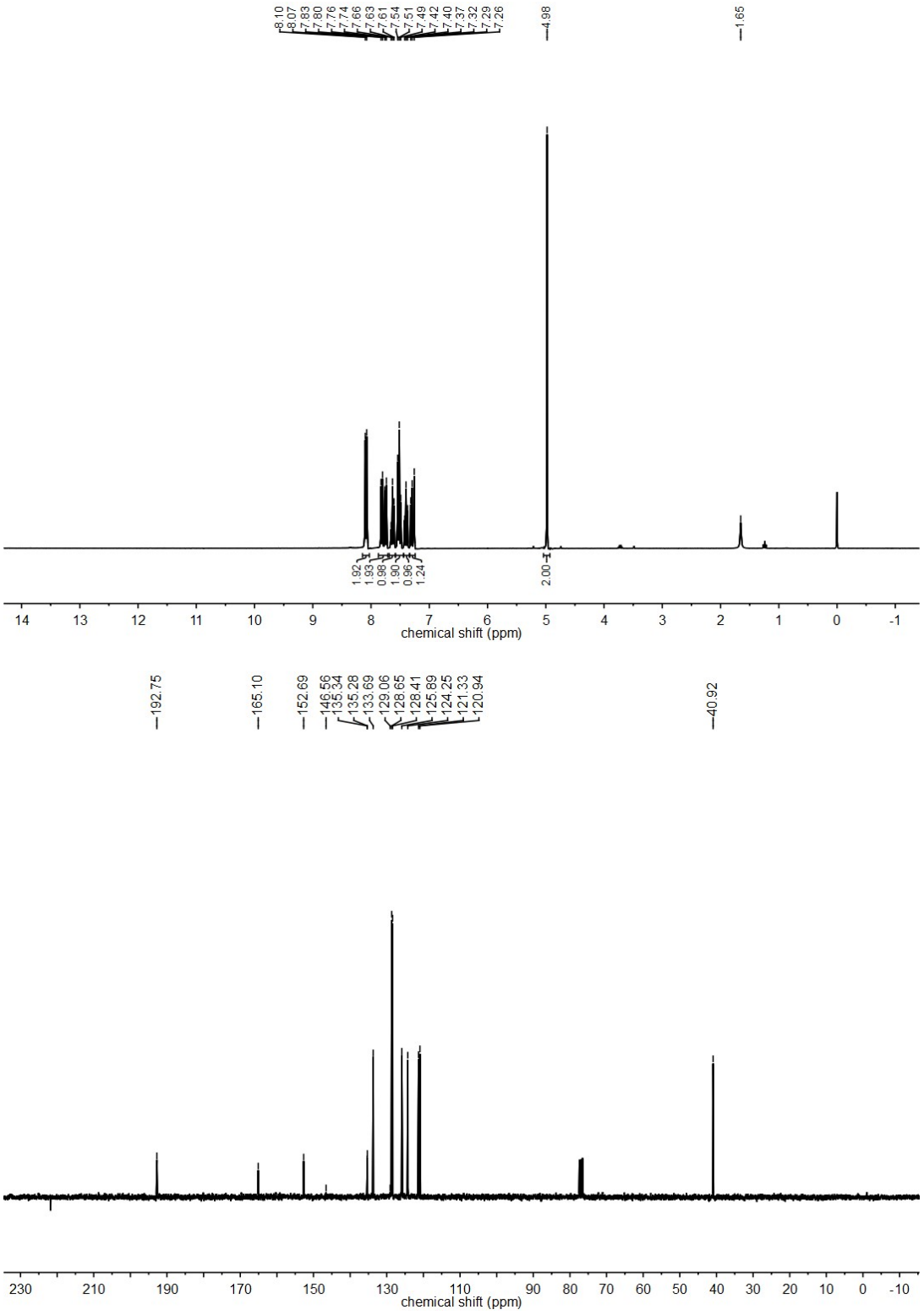

Figure S8. ^{1} **H NMR** and ^{13} **C NM**R spectrum of 2-(benzo[d]thiazol-2-ylthio)-1-(4-fluorophenyl)ethenone

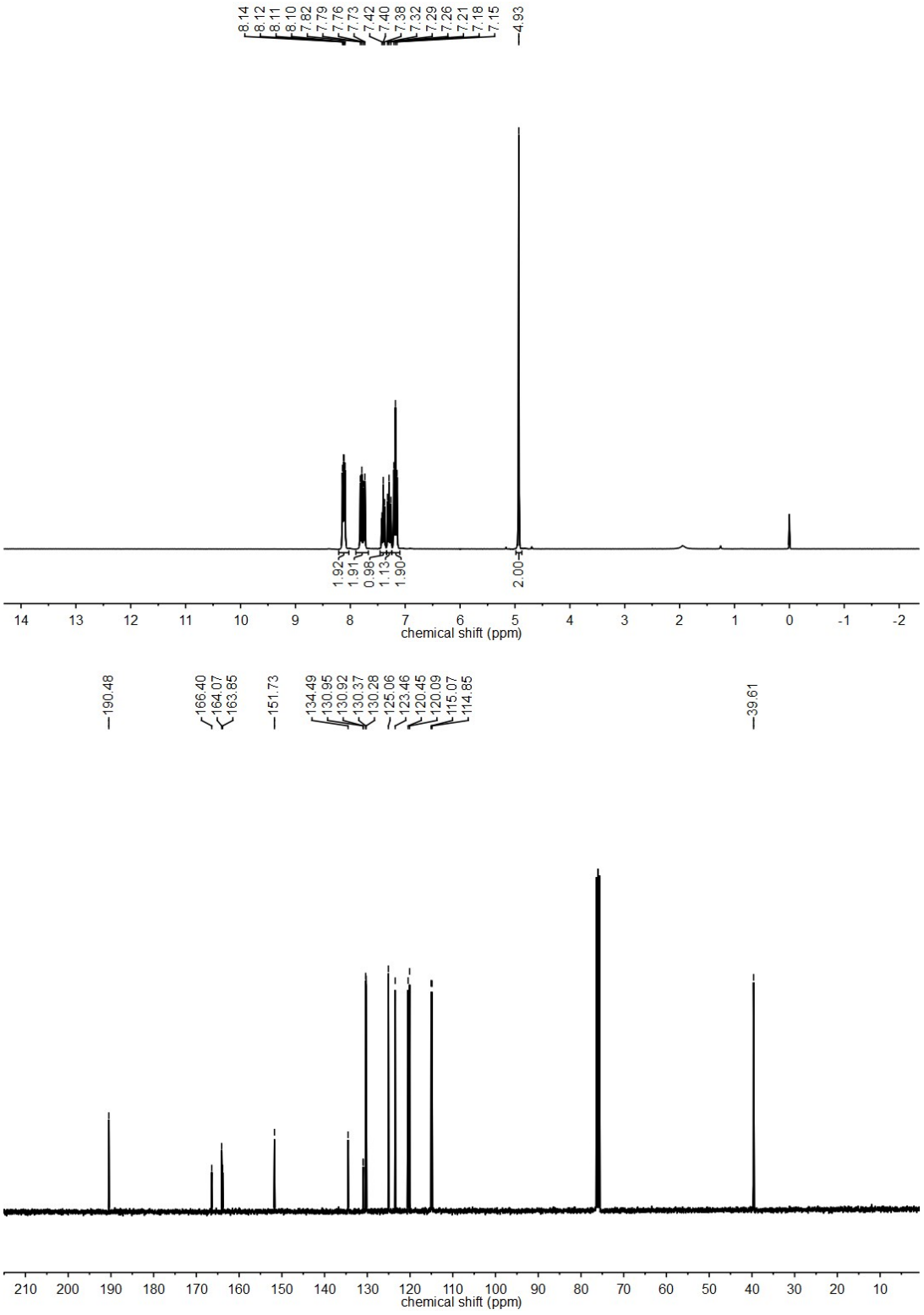

Figure S9. ^{1}H NMR and **^{13}C NM**R spectrum of 2-(benzo[d]thiazol-2-ylthio)-1-(4-chlorophenyl)ethenone

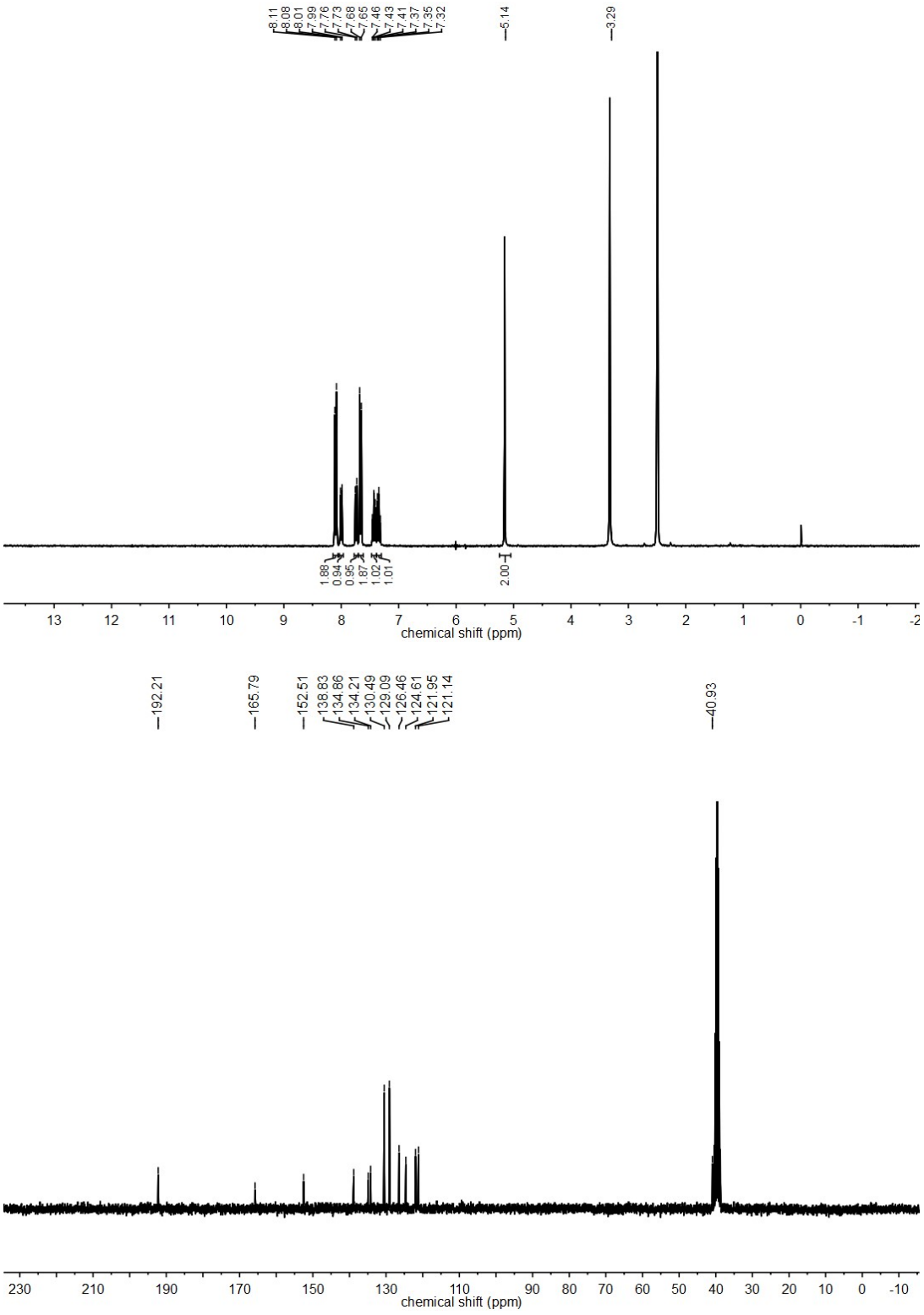

Figure S10. ^{1}H NMR and **^{13}C NM**R spectrum of 2-(benzo[d]thiazol-2-ylthio)-1-(4-bromophenyl)ethanone

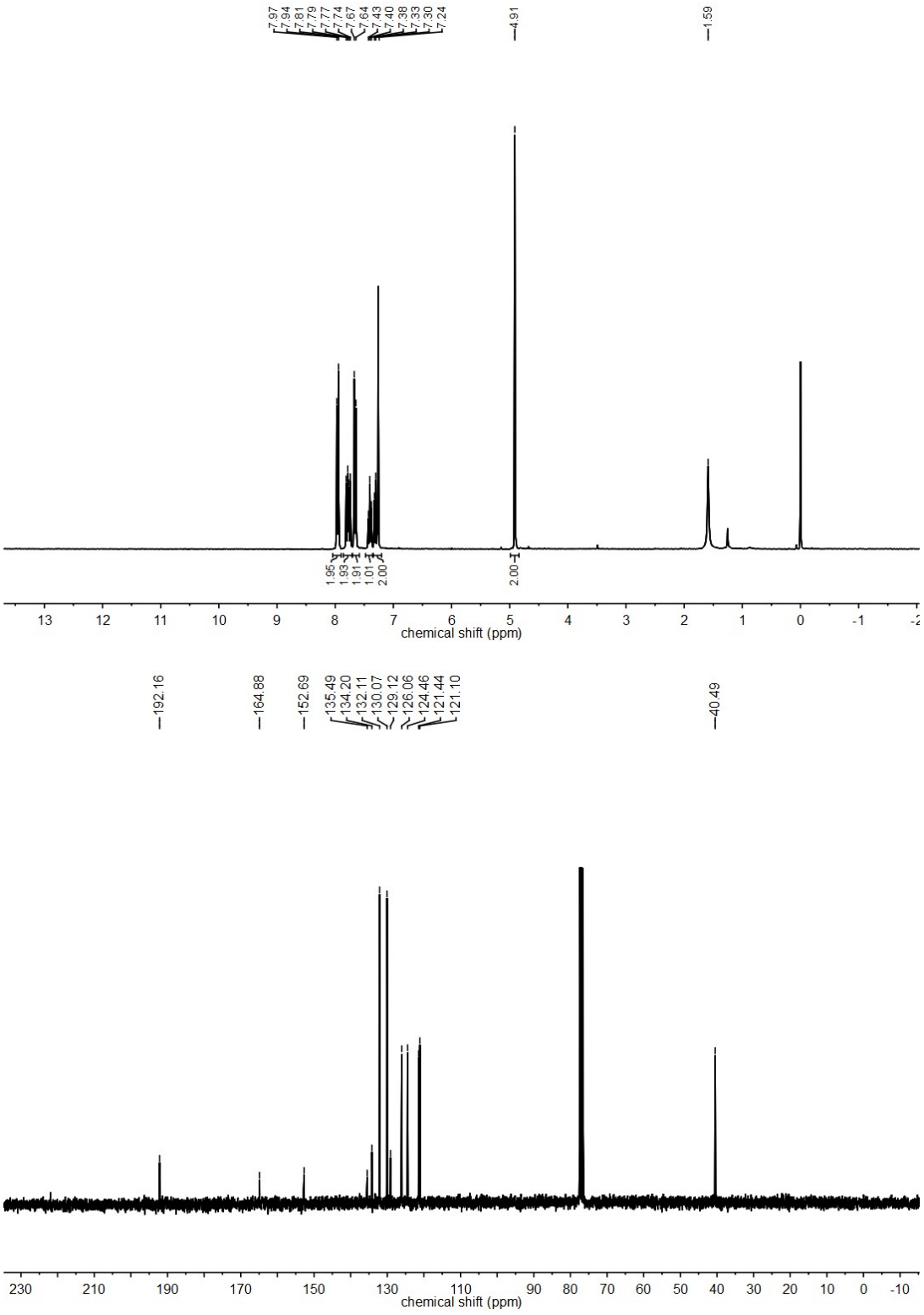

Figure S11. ^{1}H NMR and **^{13}C NM**R spectrum of 2-(benzo[d]thiazol-2-ylthio)-1-p-tolylethanone

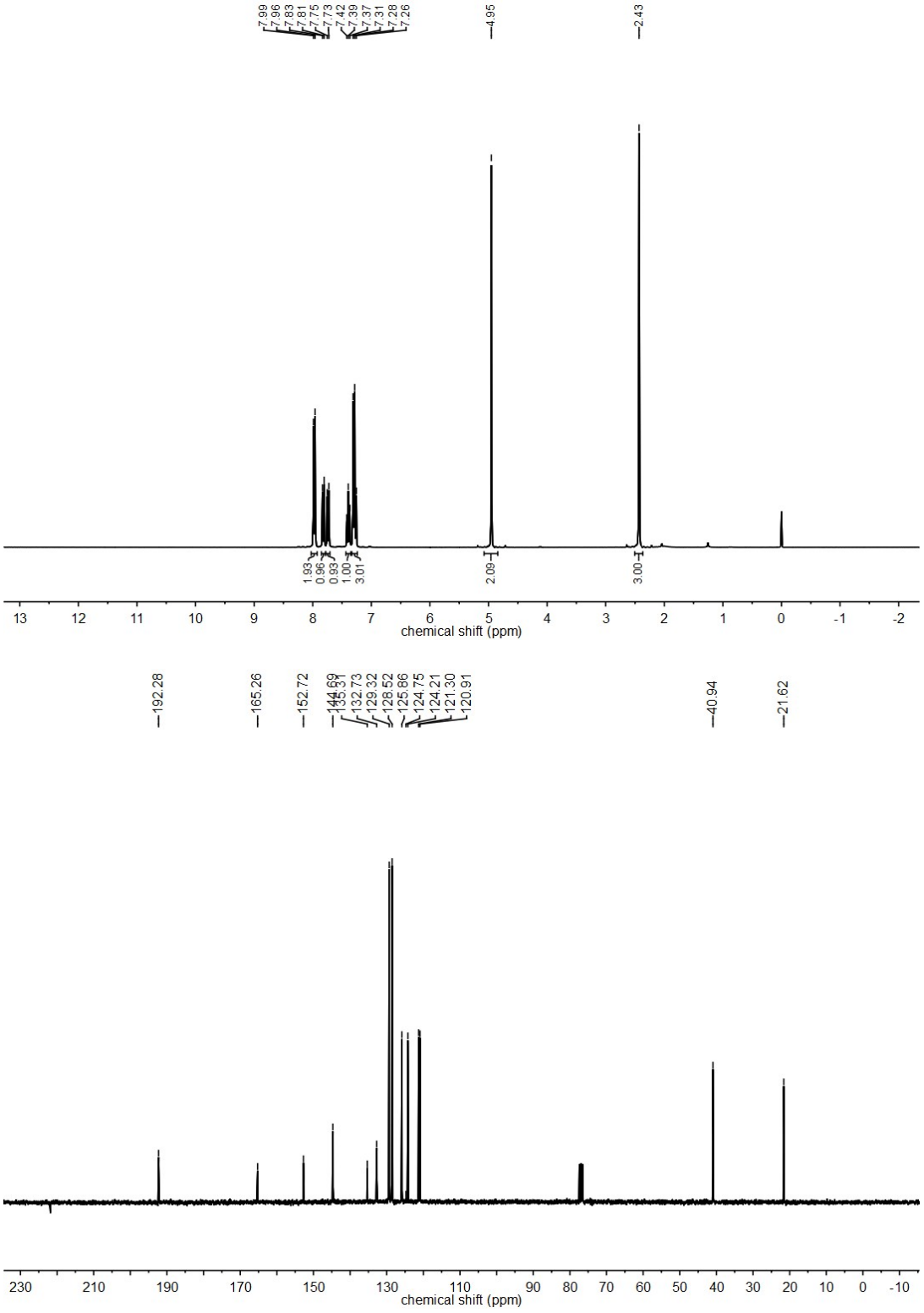

Figure S12. ^{1}**H NMR** and ^{13}**C NM**R spectrum of 2-(benzo[d]thiazol-2-ylthio)-1-(4-methoxyphenyl) ethenone

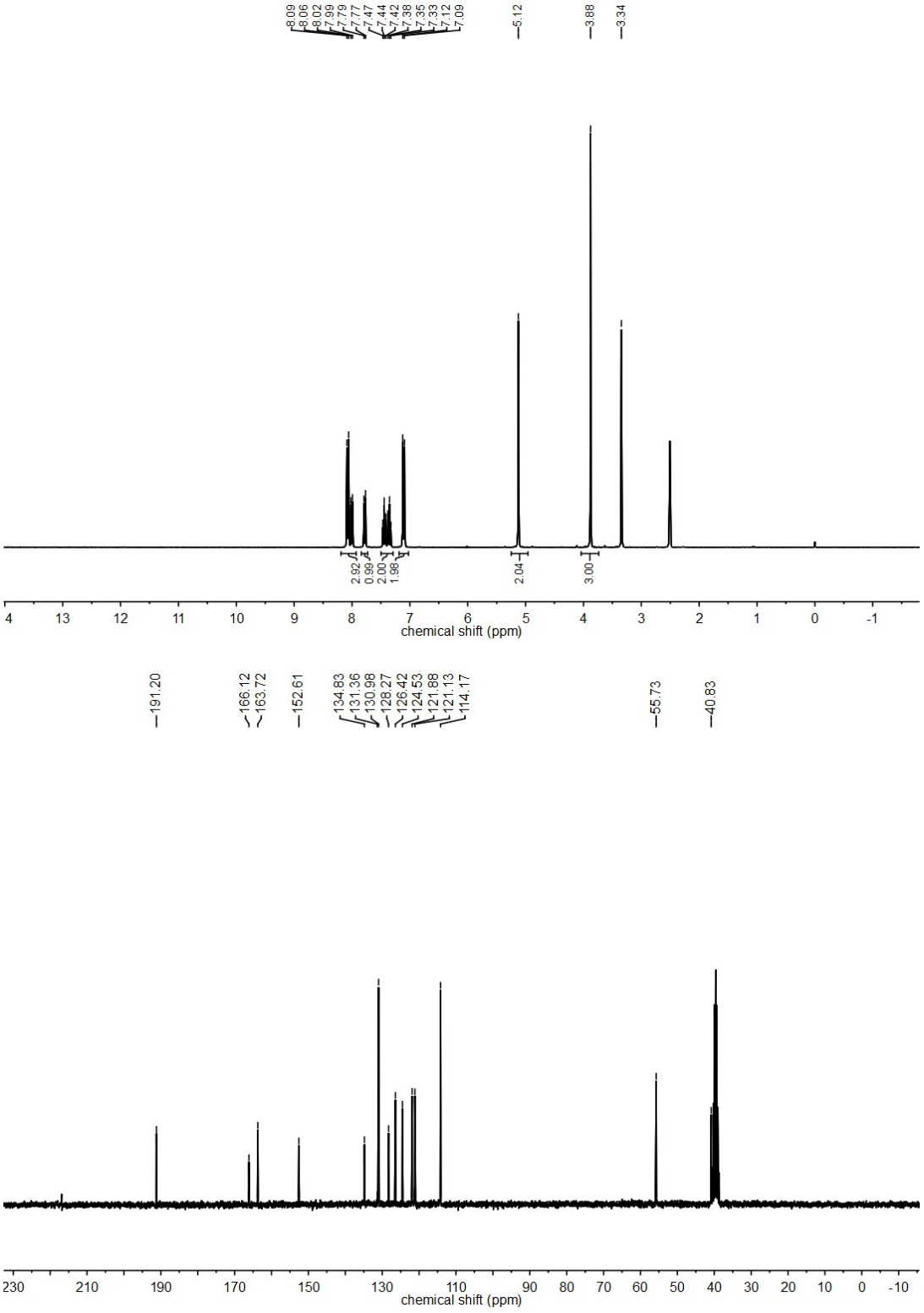

Figure S13. ^{1}**H NMR** and ^{13}**C NM**R spectrum of 1-([1,1'-biphenyl]-4-yl)-2-(benzo[d]thiazol-2-ylthio) ethenone

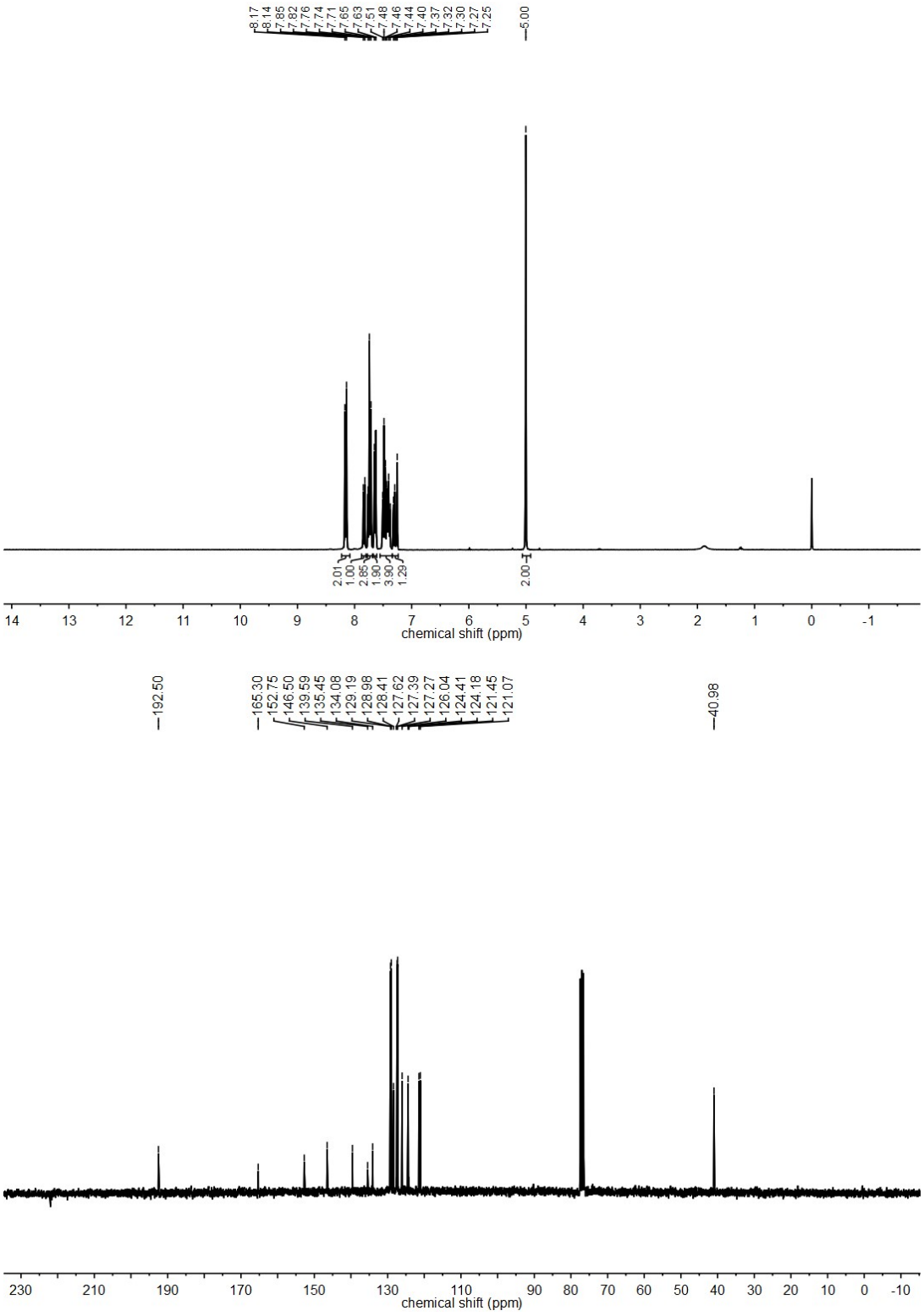

Figure S14. ^{1}H NMR and **^{13}C NM**R spectrum of 2-(4-methylbenzo[d]thiazol-2-ylthio)-1-phenylethanone

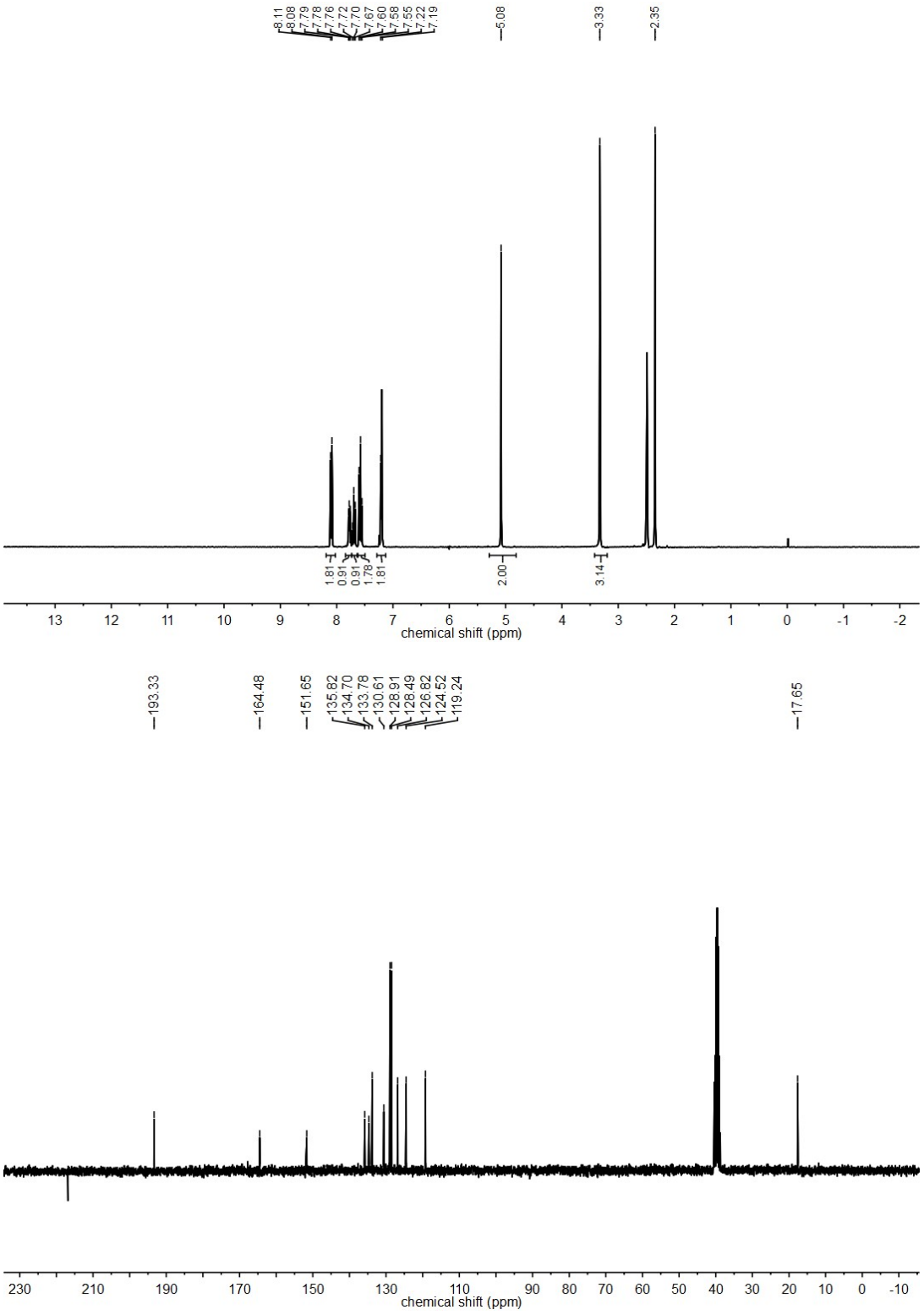

Figure S15. ^{1}H NMR and **^{13}C NM**R spectrum of 2-(5-bromobenzo[d]thiazol-2-ylthio)-1-phenylethanone

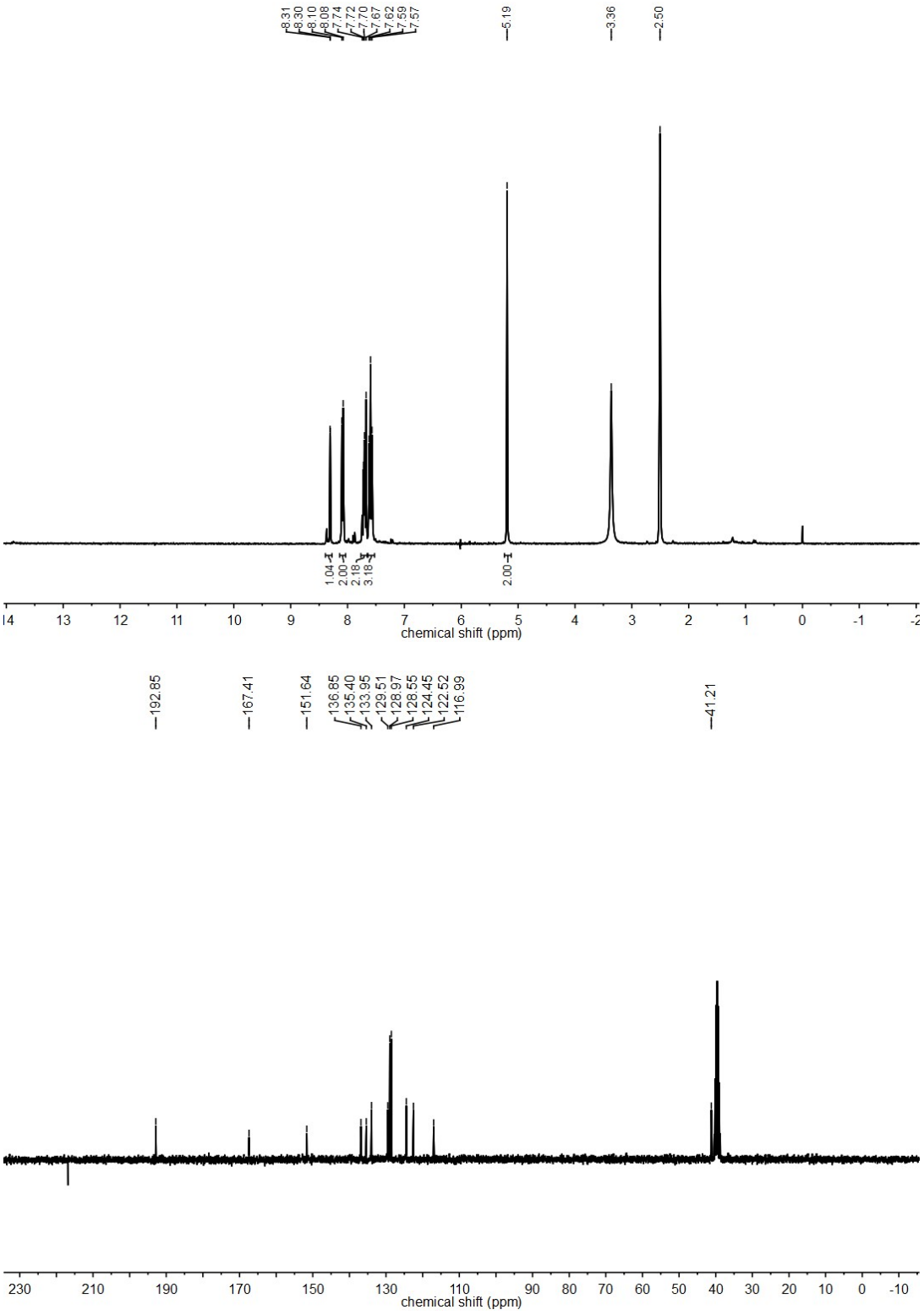

Figure S16. IR spectrum of **$[H_2L]Br_2$**

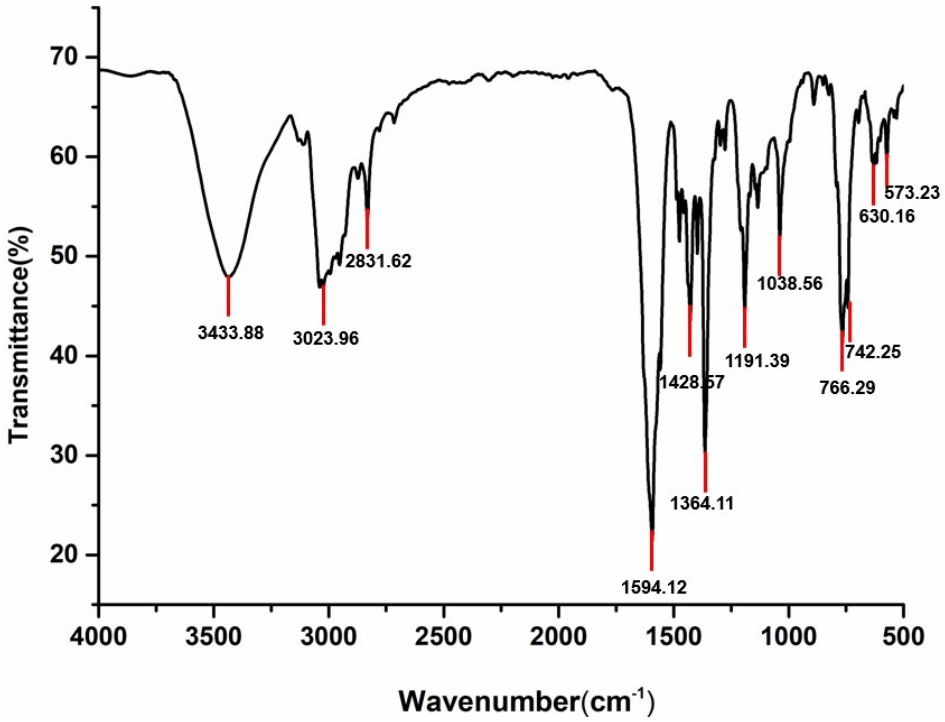

Figure S17. IR spectrum of **$[H_2L](PF_6)_2$**

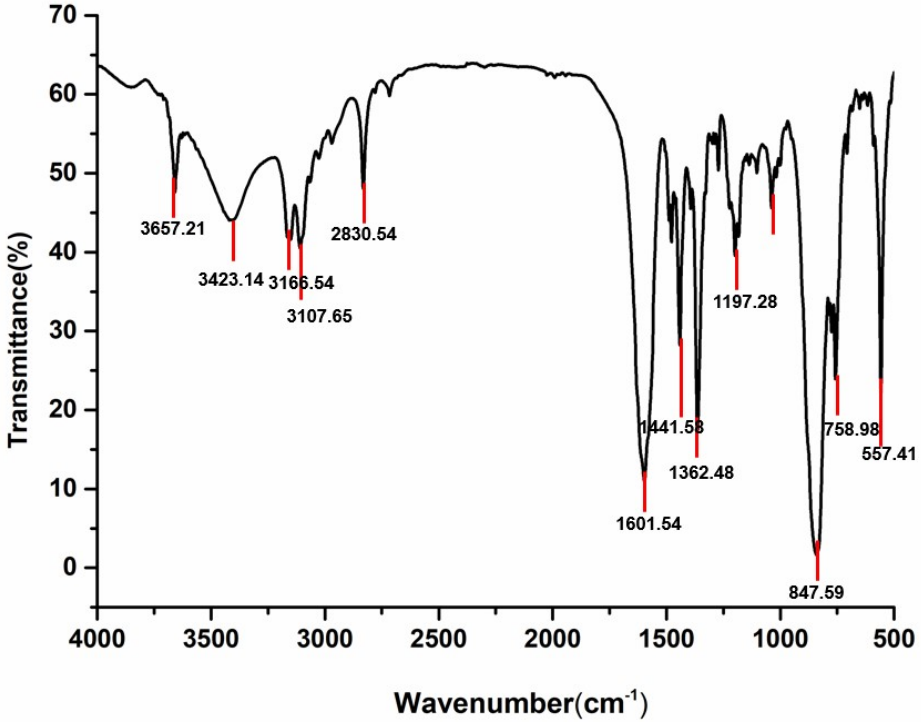

Figure S18. IR spectrum of **[NiL]Br_2·CH_3OH (1)**

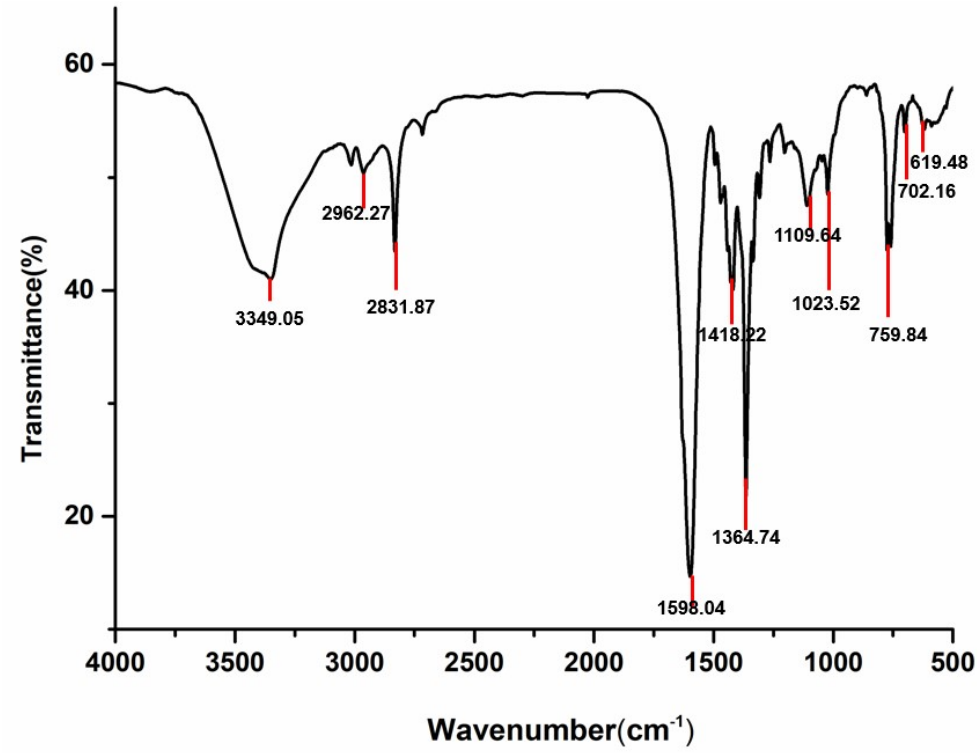

Figure S19. IR spectrum of **[NiL]$(PF_6)_2$·0.5CH_3CN (2)**

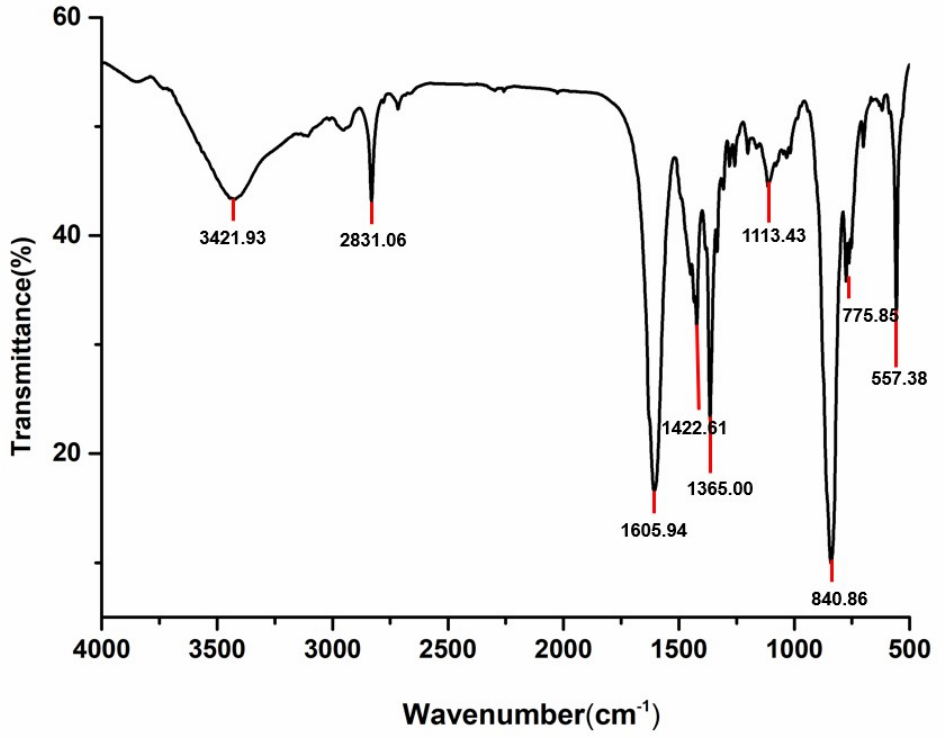

Figure S20. IR spectrum of **[NiLBr]PF_6 (3)**

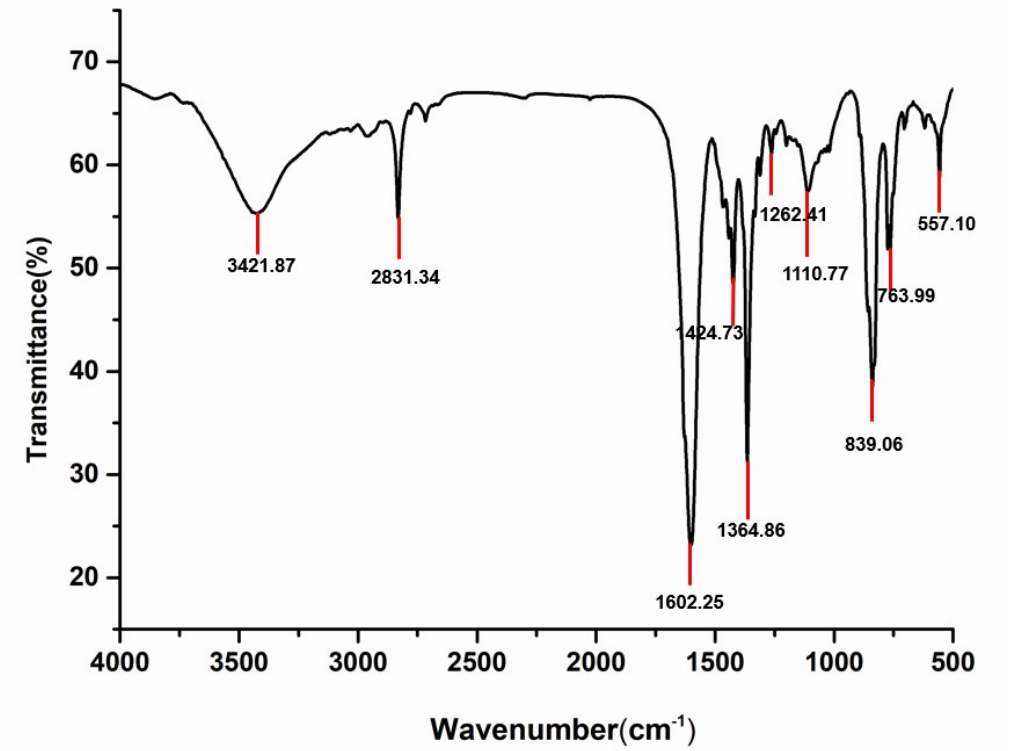

Figure S21. IR spectrum of 2-(benzo[d]thiazol-2-ylthio)-1-phenylethanone

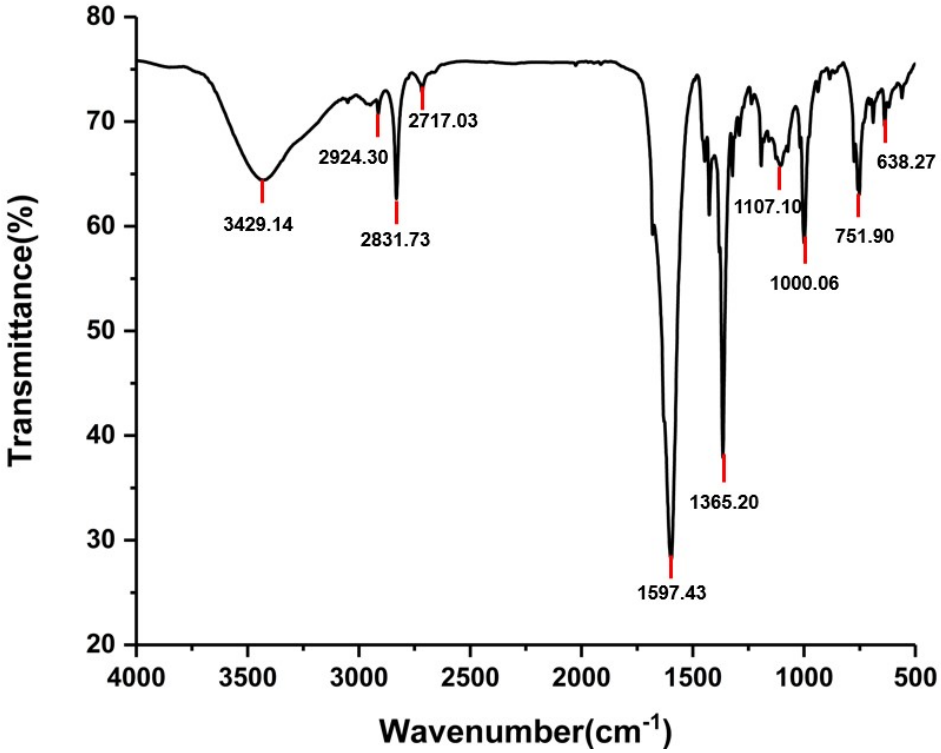

Figure S22. IR spectrum of 2-(benzo[d]thiazol-2-ylthio)-1-(4-fluorophenyl)ethenone

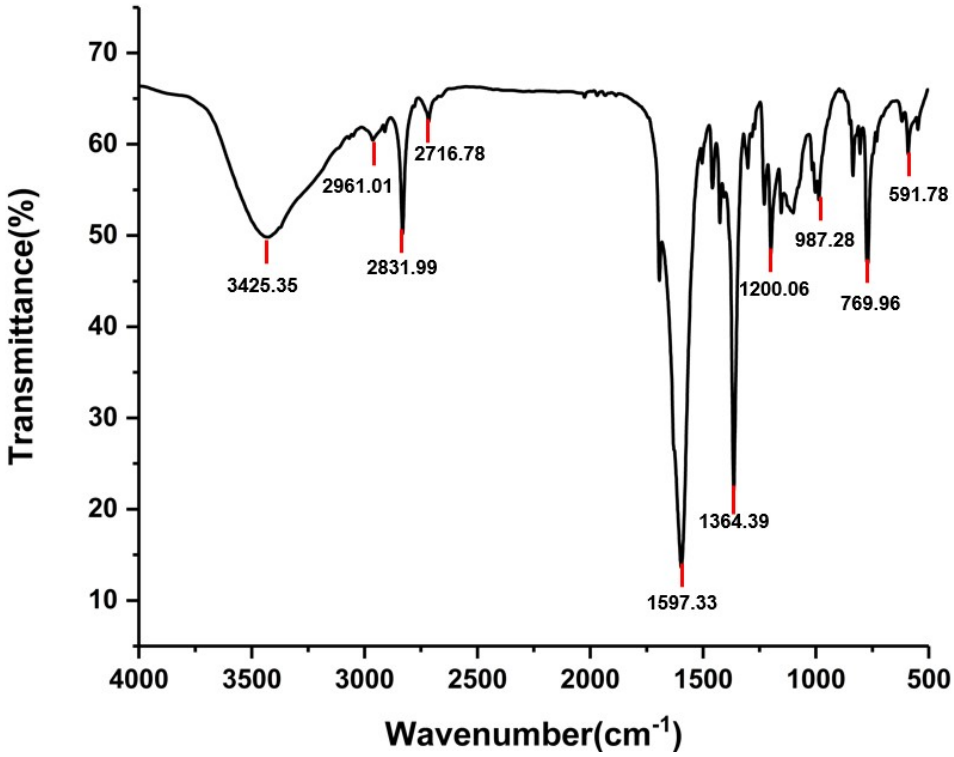

Figure S23. IR spectrum of 2-(benzo[d]thiazol-2-ylthio)-1-(4-chlorophenyl)ethenone

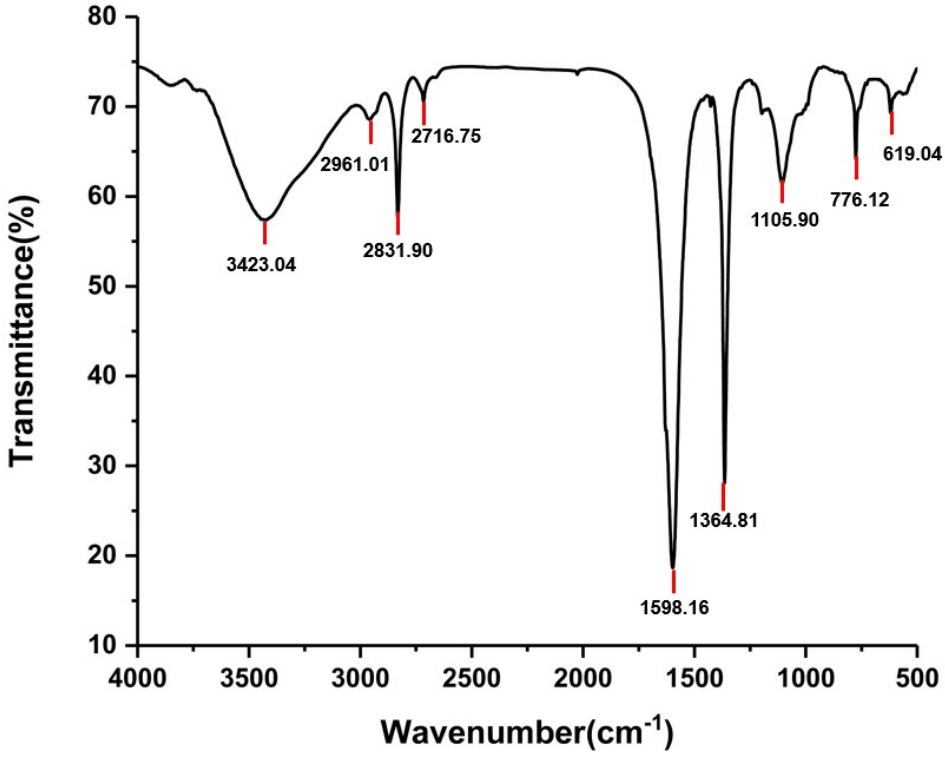

Figure S24. IR spectrum of 2-(benzo[d]thiazol-2-ylthio)-1-(4-bromophenyl)ethenone

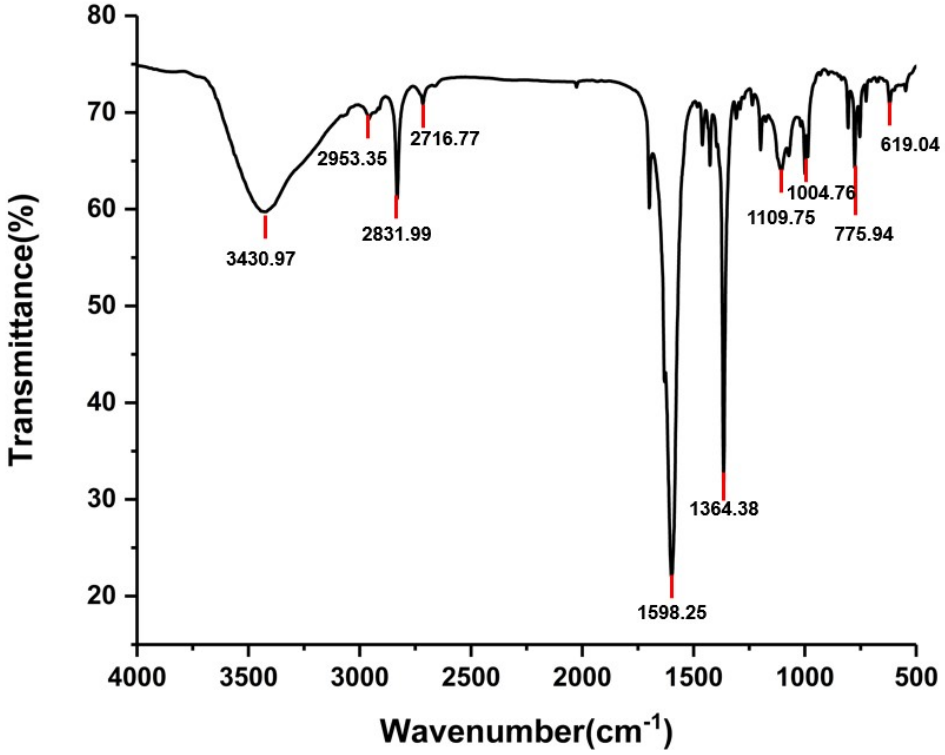

Figure S25. IR spectrum of 2-(benzo[d]thiazol-2-ylthio)-1-p-tolylethanone

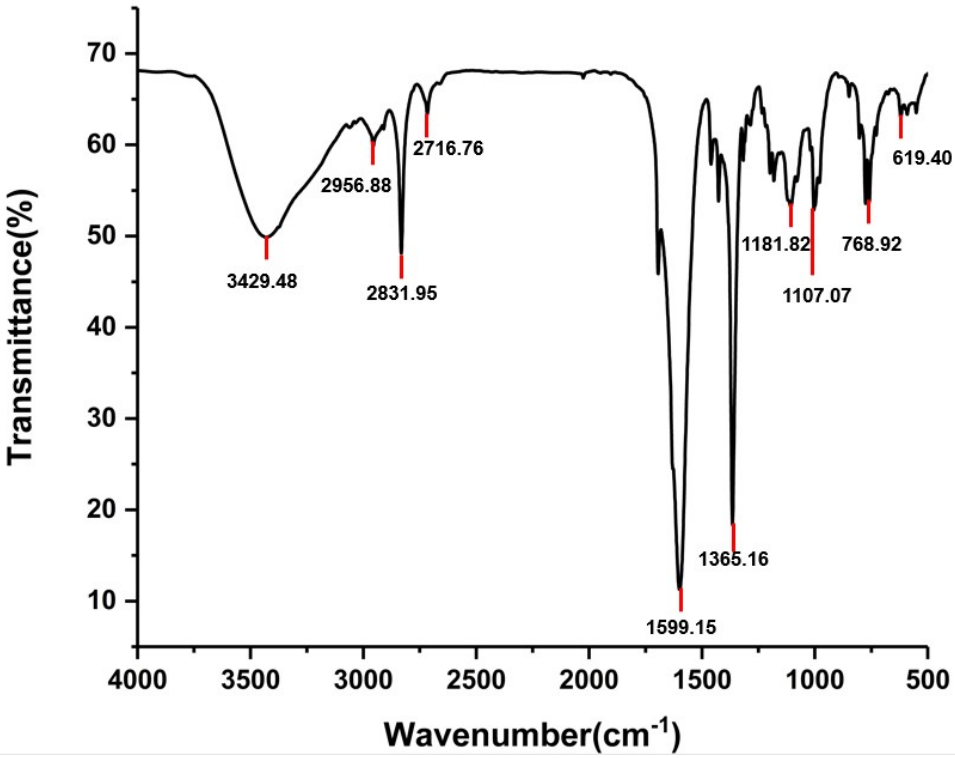

Figure S26. IR spectrum of 2-(benzo[d]thiazol-2-ylthio)-1-(4-methoxyphenyl)ethenone

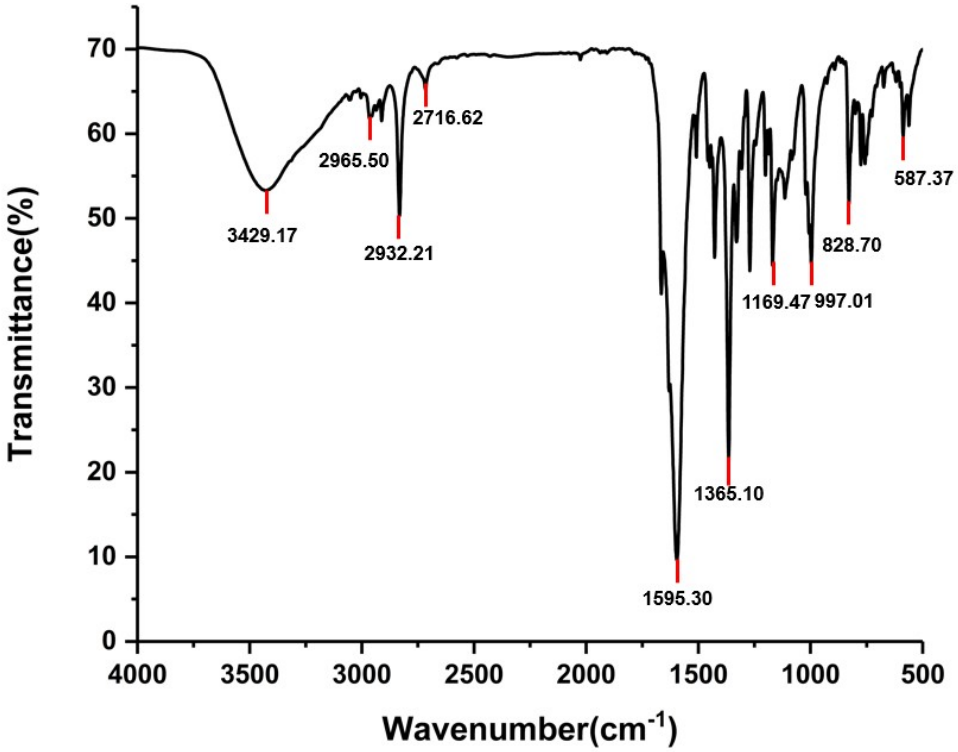

Figure S27. IR spectrum of 1-([1,1'-biphenyl]-4-yl)-2-(benzo[d]thiazol-2-ylthio)ethanone

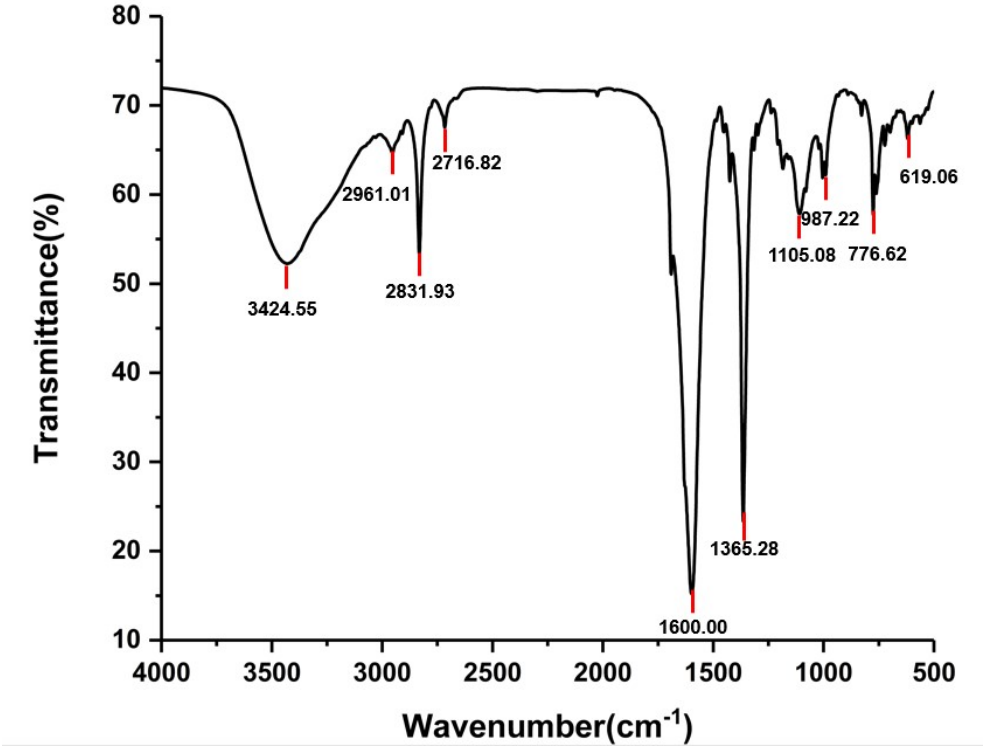

Figure S28. IR spectrum of 2-(4-methylbenzo[d]thiazol-2-ylthio)-1-phenylethanone

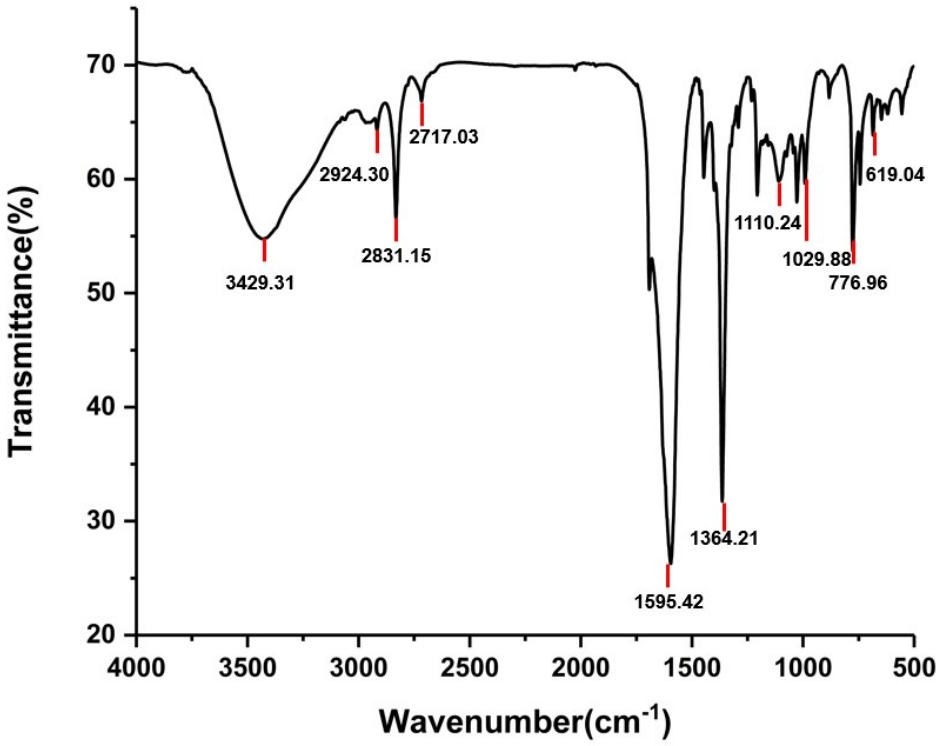

Figure S29. IR spectrum of 2-(5-bromobenzo[d]thiazol-2-ylthio)-1-phenylethanone